Lawrence Berkeley National Laboratory
Recent Work

Title

THE PREDICTION OF TEE PENETRATION DISTANCE OF PARTICUIATE GROUTS IN A POROUS MEDIUM

Permalink

https://escholarship.org/uc/item/2tc4k4tb

Author

Thomson, N.A.

Publication Date

1981-07-01

Lawrence Berkeley Laboratory
UNIVERSITY OF CALIFORNIA

ENERGY & ENVIRONMENT DIVISION

THE PREDICTION OF THE PENETRATION DISTANCE OF
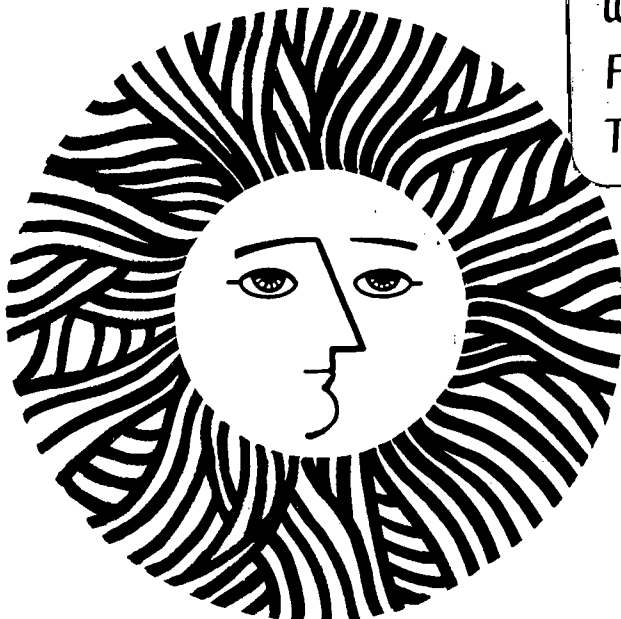PARTICULATE GROUTS IN A POROUS MEDIUM

Neil A. Thomsen
(M.S. thesis)

July 1981

DISCLAIMER

THE PREDICTION OF THE PENETRATION DISTANCE OF PARTICULATE GROUTS IN A POROUS MEDIUM

Neil A. Thomsen

CE 299 Report
Submitted for completion of requirements
for the degree of
Master of Engineering
in the Geological Engineering Group
University of California, Berkeley

July 15, 1981

Energy and Environment Division
Lawrence Berkeley Laboratory
University of California
Berkeley, California 94720

THE PREDICTION OF THE PENETRATION DISTANCE OF PARTICULATE GROUTS IN A POROUS MEDIUM

Contents

LIST OF SYMBOLS

a	capillary cross-sectional area (L^2)*
A	porous medium cross-sectional area (L^2)
b	number of tubes in bundle of tubes
B	Bingham fluid abbreviation
C	Casson fluid abbreviation
C	Thomsen pore shape factor (dimensionless)
C_o	Kozeny-Carman pore shape factor (dimensionless)
C_s	shape coefficient (dimensionless)
dV/dy	shear rate (1/T)
e	void ratio (L^3/L^3)
f	fractional flow rate (L^3/T)
G	pressure gradient $(F/L^2/L)$
G_c	critical pressure gradient $(F/L^2/L)$
H	hydraulic head (L)
H-B	Herschel-Bulkley fluid abbreviation
i	hydraulic gradient (L/L)
i_c	critical hydraulic gradient for non-Newtonian flow (L/L)
k	coefficient of intrinsic permeability (L^2)
K	coefficient of hydraulic conductivity (L/T)
L	distance (L)
L_{max}	maximum distance of penetration of non-Newtonian fluid in a capillary or a porous medium (L)

---

* Fundamental units are F-force, L-length, T-time.

n	porosity (L^3/L^3)
N	ratio of grout kinematic viscosity to water kinematic viscosity (dimensionless)
P	wetted perimeter (L)
P	pressure (F/L^2)
P_i	injection pressure (F/L^2)
P_o	in situ pressure (F/L^2)
Q	flow rate (L^3/T)
r	radius (L)
r_c	radius of unsheared cylinder (L)
r_o	radius of grout injection tube (L)
R	radius of circular tube (L)
R_H	hydraulic radius defined as ratio of area of flow to wetted perimeter (L)
R_{min}	radius of smallest pore that can be penetrated by non-Newtonian grout (L)
S	saturation (L^3/L^3)
S_o	specific surface of grains per unit volume (1/L)
t	time (T)
T	coefficient of tortuosity (dimensionless)
V	volume (L^3)
V	velocity (L/T)
v	Darcy velocity (L/T)
x	distance (L)
y	height (L)

Greek Letters

γ specific weight (F/L^3)

μ absolute viscosity $(F\ T/L^2)$

ν kinematic viscosity (L^2/T)

τ shear stress (F/L^2)

τ_w shear stress developed at tube wall (F/L^2)

τ_y yield strength of non-Newtonian fluid (F/L^2)

I. INTRODUCTION

The purpose of this report is to develop a method for predicting the maximum penetration distance of a particulate grout into a porous medium. Since particulate grouts usually have non-Newtonian fluid properties, it is this particular aspect of the problem that will be our main concern. When grouts are injected into a porous medium under a certain injection pressure the grout flow or "take" decreases from some initial value to zero. This means that the radius of the grouted mass must grow to some maximum size for a given injection pressure. The grouted mass radius in turn determines the maximum hole spacing for a grouting project. The maximum hole spacing is usually the most important parameter in determining the cost of a grouting project since the amount of grout required is determined by the porosity of the medium which is usually fairly well known. Therefore, if some method were available for predicting the penetration distance of grouts then the maximum hole spacing for grouting projects could be rationally estimated and better cost estimates could be prepared.

This report is divided into two parts. Part I contains the development of a conceptual model and a proposed formula for prediction of penetration distances. In this section grout fluid properties are examined, previous work is presented and analyzed, the applicability of Darcy's Law to grout flow is discussed, and a hypothesis is presented for predicting the penetration distance. The second part contains the results of laboratory testing of the hypotnesis carried

out by the author at LBL. Interpretation and conclusions of the results are presented.

Although there are many practical applications of a method for predicting the size of a grouted mass formed during grouting, this particular report is a result of the Lawrence Berkeley Laboratory's evaluation of barrier options for abandoned modified in-situ oil shale retorts in Western Colorado. Adverse environmental effects of oil shale development by modified in-situ retorting include groundwater degradation due to leaching of in-situ spent shale and subsidence of retort overburden. Low resources recovery is an additional problem because of the need to leave large pillars of intact raw shale in place to support overburden. One possible solution to all three of these problems is backfilling abandoned retorts with a grout containing a large proportion of surface-retorted shale. Development of a low-cost grout based on surface-retorted shale has also been investigated at LBL.

The abandoned retort consists of a packed chamber of rubble with a complex void distribution. Voids include spaces between pieces of rubble, which may range from fines to boulders, fractures along the bedding plane in individual pieces of shale, and micropores created by the pyrolysis of kerogen. The introduced grout must uniformly penetrate and fill a majority of the large voids to achieve low hydraulic conductivity in the retort. This may be achieved if a sufficiently large number of closely spaced drill holes are used or if the grout fluid properties are especially favorable for wide-spread distribution

from an individual drill hole. An economic tradeoff exists between

the cost of drill holes and the costs of providing a suitable grout.

Since retorts are deep--1000 to 2000 ft deep--drilling grout injection

holes will be costly. However, use of grout additives to produce a

favorable grout will also be costly.

II. THEORETICAL DEVELOPMENT OF HYPOTHESIS FOR PREDICTION OF PENETRATION DISTANCE IN A POROUS MEDIUM

A. Discussion of the Fluid Characteristics of Particulate Grouts

Particulate grouts--such as cement and clay grouts--usually exhibit non-Newtonian fluid behavior. In general, fluid behavior is usually characterized by the relationship between shear stress, τ, developed in the fluid by a given rate of shear or velocity gradient, dV/dy, for Couette-type flow. If the apparent viscosity of a fluid is defined as:

$$\text{apparent viscosity} = \frac{\tau}{dV/dy} = \mu_{ap} \tag{1}$$

and the absolute or differential viscosity is defined as:

$$\text{absolute viscosity} = \frac{d\tau}{d^2V/dy^2} = \mu_{abs} \tag{2}$$

then by definition a Newtonian fluid satisfies the following condition:

$$\mu_{ap} = \mu_{abs}$$

Graphically (see Fig. 1) we see that the slope of the flow curve for a Newtonian fluid is a constant and intersects the ordinate axis at $\tau = 0$. Any fluid that does not satisfy the above conditions is by definition a non-Newtonian fluid. Since most fluid mechanics applications deal only with Newtonian fluids the distinction between

absolute and apparent viscosity is not usually explicitly stated. However, for non-Newtonian fluids the distinction is very important.

In addition to being non-Newtonian fluids, particulate grouts also possess a "yield strength"--τ_y. For Couette flow the yield strength is that value of shear stress that must be applied before the fluid will flow. In other words, as Fig. 1 shows, the flow curves for these fluids intercept the ordinate axis at a non-zero value--τ_y. Table 1 gives the rheological models commonly used to fit viscometer data relating shear stress and shear rate for various types of fluids. Cement and clay grouts, as well as many other slurries and plastics, usually behave like Bingham, Casson, or Herschel-Bulkley fluids. These fluids all have a non-zero yield strength and, therefore, will be examined in this report. Throughout this report these fluids will be abbreviated as B, C, or H-B fluids, respectively.

As with Newtonian fluids the flow curves for particulate grouts also vary with temperature and pressure for a given fluid. Thus, fluid parameters should be referred to a given temperature and pressure for comparison. In this report isothermal conditions are assumed. The change in fluid properties due to changing pressures is insignificant.

The properties and rheological equations of these particular non-Newtonian fluids are independent of time. An additional group of non-Newtonian fluids which exhibit thixotropic or rheopectic behavior have properties that do depend on time and stress history. Thixotropic fluids suffer a substantial loss of strength after vigorous shaking

Table 1. Rheological equations for Newtonian and some non-Newtonian
          fluids.

Fluid	Rheological Equation	Remarks
Newtonian	$\tau = \mu(dV/dy)$	μ = constant
Pseudo-Plastic	$\tau = p(dV/dy)^{r}$	P and r = constants; r < 1
Dilatant	$\tau = M(dV/dy)^{q}$	M and q = constants; q > 1
Bingham	$\tau = \tau_{y} + \mu_{B}(dV/dy)$	τ_{y} and μ_{B} are constants
Casson	$\sqrt{\tau} = \sqrt{\tau_{y}} + \sqrt{\mu_{c}(dV/dy)}$	τ_{y} and μ_{c} are constants
Herschel-Bulkley	$\tau = \tau_{y} + J(dV/dy)^{1/m}$	τ_{y}, J, and m are constant; m > 1

but regain strength if allowed to rest for a period of time. Also, if a thixotropic fluid is sheared at a fixed rate for a period of time the shear stress developed in the fluid decreases (Wilkinson, 1960). Rheopectic fluids exhibit behavior opposite to that of thixotropic fluids, that is, the shear strength of the fluid increases with continued shearing. Most particulate grouts exhibit pronounced thixotropic behavior, whereas no grout appears to exhibit rheopectic behavior.

Thixotropic and rheopectic fluids are difficult to mathematically characterize and no widely accepted rheological equations have been proposed to describe these fluids (Wilkinson, 1960; Skelland, 1967). However, thixotropic fluids behave as either Newtonian fluids or as time-independent non-Newtonian fluids for a period of time after vigorous shaking or mixing. Therefore, in the limiting case, thixotropic fluids can be characterized using rheological equations for time-independent fluids as long as it is realized the time-independent model is applicable only for a given time interval and a given stress history.

B. Flow of Non-Newtonian Fluids with Yield Strength in Circular, Horizontal Tubes

Figure 2 gives the laminar flow relationships for a Newtonian fluid in a straight, circular, horizontal tube under steady state conditions. According to Poiseuille's Law, for these conditions the flow rate = $Q = 0$ when the pressure gradient = $dP/dx = 0$. This is contrasted with non-Newtonian fluid flow with the same conditions. Consider a

cylindrical element in a fluid flowing in a pipe. This element is shown in Fig. 3. When flow is from left to right, that is, $P_1 > P_2$ then the overall force balance for constant velocity is

$$P_1 \pi r^2 = \tau\, 2\pi r\, L + P_2 \pi r^2$$

or

$$\frac{P_1 - P_2}{L}\, \frac{r}{2} = \tau = \tau(r) \qquad (3)$$

The differential form of this equation is, of course,

$$\frac{dP}{dL}\, \frac{r}{2} = \tau(r) \qquad (4)$$

The shear stress developed across the tube is shown diagrammatically in Fig. 4. Since $dV/dr = 0$ at $r = 0$ then $\tau(0) = 0$ for a Newtonian fluid and $\tau(0) \leq \tau_y$ for a non-Newtonian fluid with a yield strength (see Fig. 1). Therefore, as is shown in Fig. 4 for non-Newtonian fluids flowing in straight, circular, horizontal tubes, an unsheared cylinder develops in the center of the tube, that is, the cylinder travels at a constant velocity but is not being sheared as is the material between the cylinder and the tube wall. For a fluid of given yield strength and under a given pressure gradient the radius of the the unsheared cylinder is

$$r_c = 2\tau_y / (dP/dL) = \frac{2\tau_y}{G}$$ (5)

wnere $G = dP/dL = $ pressure gradient. This result is obtained by solving Eq. (4) and recognizing that

$$\tau(r_c) = \tau_y$$ (6)

The velocity of the unsheared cylinder for a Bingham Fluid is given by (Hughes, 1979)

$$V_c = \frac{\tau_y^2}{\mu_B G} \left(\frac{R}{r_c} - 1\right)^2$$ (7)

Obviously, if $r_c = R = $ the radius of the tube, then flow must cease since no shear deformation is occurring within the fluid or between the fluid and the tube wall.

Another way of looking at the pecularities of non-Newtonian fluid flow is to consider flow between two reservoirs connected with a straight, circular, horizontal tube of radius R and length L as shown in Fig. 5. Furthermore, let us assume the fluid tested is a Bingham fluid with constitutive equation

$$\tau = \tau_y + \mu_B (dV/dr)$$

For steady state flow with H_1 and H_4 constant the rate of flow between the two reservoirs is

$$Q = \frac{\pi R^4 G}{8\mu_B} \left[1 - \frac{4}{3}\left(\frac{2\tau_y}{RG}\right) + \frac{1}{3}\left(\frac{2\tau_y}{RG}\right)^4 \right] \qquad (8)$$

where

$$G = \frac{\gamma(H_1 - H_4)}{L} = \text{pressure gradient (Hughes, 1979)} \quad .$$

Furthermore, an unsheared cylinder exists within the tube as discussed in the preceding paragraph. The radius of this solid cylinder is

$$r_{c1} = \frac{2\tau_y}{G} = \frac{2\tau_y L}{\gamma(H_1 - H_4)}$$

Note that this solid sylinder extends along the complete length of the tube, that is, r_{c1} is constant from the tube inlet to tube outlet. If the height of Bingham fluid in the inlet reservoir is lowered to H_2 the rate of flow–Q–decreases and the radius of the solid cylinder will increase to

$$r_{c2} = \frac{2\tau_y L}{\gamma(H_2 - H_4)} > r_{c1} \quad \text{since} \quad H_2 < H_1 \quad .$$

Obviously, since this is a linear relationship, for a given Bingham fluid with fluid properties τ_y and γ there must be some height of fluid $H_3 > H_4$ where

$$r_c = \frac{2\tau_y L}{\gamma(H_3 - H_4)} = R \quad . \tag{9}$$

Again we see that flow must cease when $H = H_3$ since the tube is now filled with an unsheared solid cylinder. The pressure gradient at which flow ceases is defined as

$$G_c = \text{critical pressure gradient} = \frac{2\tau_y}{R}$$

and occurs when $r_c = R$. Also we can see that by substituting

$$r_c = R = \frac{2\tau_y}{G_c}$$

into Eq. (8) we obtain $Q = 0$ and substituting into Eq. (7) we obtain $V_c = 0$. Therefore, flow of a Bingham fluid through a tube as shown in Fig. 5 must cease at some non-zero pressure gradient and the shear stress developed along the tube wall when flow ceases must be τ_y. This is completely different than the case of a Newtonian fluid where flow ceases only when the pressure gradient is zero. It is important to note that the non-zero pressure gradient required to obtain $Q = 0$ is not dependent on the absolute viscosity of the Bingham fluid. Although the above argument has been presented for a Bingham fluid it also holds true for any non-Newtonian fluid with a yield strength since the crucial step is Eq. (5) which holds true for Casson and Herschel-Bulkley fluids as well. For these other fluids the cylinder velocity

and flow rate equations are different from Eqs. (7) and (8) but flow still ceases at a non-zero pressure gradient which is only a function of the yield strength and tube radius.

An important consequence of the above discussion is that it is possible to predict the maximum penetration distance of a non-Newtonian grout into a straight, horizontal, circular tube. This follows from Eq. (9) when we consider the schematic set-up shown in Fig. 6 which is a variation of that shown in Fig. 5. In Fig. 6, the left reservoir is filled with a non-Newtonian grout of fixed pressure head H_g and the tube, of length L_f and radius R, is initially filled with water of fixed pressure head H_w such that $H_g > H_w$. When the valve at A is opened and the grout flows into the tube, water will be displaced and overflow the right hand reservoir. At any given instant of time t_1, when the fluids are still flowing, the pressure head at A is H_g, at B the head is H_B, and at C the head is H_w, where $H_g > H_B > H_w$. Also, at t_1 the radius of the solid, unsheared cylinder in the center of the grout is

$$r_c = \frac{L_B \, 2\tau_y}{\gamma_g (H_g - H_B)}$$

from Eq. (9) where γ_g = specific weight of the grout and L_B = distance from the left reservoir to the grout-water interface at time = t_1. This solid, unsheared cylinder extends from the grout-water interface to the left reservoir and its radius all along its length is r_c.

Obviously as the interface moves to the right the pressure gradient within the grout is

$$G_L = \frac{\gamma_g (H_g - H_L)}{L}$$

and must be constantly decreasing as L increases. This is shown schematically in Fig. 7. Thus, by examination of Eq. (9), we see that the radius of the solid, unsheared cylinder in the grout must be constantly increasing as grout flows from left to right although at any instant in time the cylinder radius is constant along the grout length. If the tube is long enough, we must reach a point where the radius of the unsheared cylinder is equal to the tube radius and flow ceases just as explained in the previous paragraphs. When flow ceases the pressure head at the stationary grout-water interface must be H_w. Therefore, the maximum penetration distance of the grout in the tube is given by

$$L_{max} = \frac{R\gamma_g (H_g - H_w)}{2\tau_y} \tag{10}$$

which is essentially Eq. (9) solved for L. Thus, for the special case of injection of a particulate grout into a straight, horizontal, circular tube Eq. (10) allows us to predict the maximum penetration distance. An important point to note with Eq. (10) is that it is the result of a fluid statics analysis, not a fluid dynamics analysis.

C. Discussion of Available Methods for Prediction of Penetration Distance of Newtonian Grout

Before examining methods for predicting the penetration distance of particulate grouts it is useful to examine theoretical procedures for predicting Newtonian grout penetration. Most chemical grouts in wide use such as AM-9, sodium silicate, and lignin sulfonate are Newtonian fluids. Therefore, examination of Newtonian penetration models may provide analogies for development of non-Newtonian grout penetration models.

The governing differential equation based on Darcy's Law for determining the location of the Newtonian grout front with respect to time was developed by S. E. Buckley and M. C. Leverett in 1942. They developed their equation for applications in the oil industry where oil or gas recovery would be increased by injecting water into a reservoir in one bore hole and displacing oil toward another bore hole where the oil would be pumped to the surface. The Buckley-Leverett equation adapted for Newtonian grouts is

$$nA \frac{\partial S_{grout}}{\partial t} + Q \frac{\partial f_{grout}}{\partial S_{grout}} \frac{\partial S_{grout}}{\partial x} = 0 \tag{11}$$

where n = media porosity; A = cross-sectional area; S_{grout} = saturation of the medium with respect to the grout; t = time; Q = total flow rate through the medium = $Q_{grout} + Q_{water}$; f_{grout} = fractional flow rate of grout at a given S_{grout}, i.e., $f_{grout} = Q_{grout}/Q$; and x = distance from injection point. The underlying assumptions for

this equation are that flow is one-dimensional and isothermal, the
medium is homogeneous and isotropic, the fluids are immiscible and
incompressible, and capillary and gravitational effects are negligible.
This differential equation can be solved using the graphical techniques
of Welge (1952) or numerical models developed by Mercer (1972). An
excellent summary of the Buckley-Leverett equation is given by Morel-
Seytous (1969) and Corey (1977). The details of these solution methods
are beyond the scope of this paper but they yield results shown
schematically in Fig. 8.

Another theoretical expression derived by Raffle and Greenwood
(1961) for a Newtonian grout injected into a water-saturated porous
medium from a spherical source and giving a spherical-shaped grouted
mass is

$$t = \frac{nr_0^2}{H_1 K} \left\{ \frac{N}{3} \left[\left(\frac{r}{r_0}\right)^3 - 1 \right] - \frac{N-1}{2} \left[\left(\frac{r}{r_0}\right)^2 - 1 \right] \right\} \tag{12}$$

where t = time duration after beginning of injection or gel time,
whichever is less; n = porosity; r_0 = radius of injection pipe; r =
radius of spherical grouted mass at time t; H_1 = injection pressure
head at tip of pipe; K = hydraulic conductivity of soil with respect
to water; and n = ratio of grout kinematic viscosity to water kinematic
viscosity. This formula was developed for use with chemical grouts.

However, the derivation of this equation contains a very important
error. Raffle and Greenwood assumed that the hydraulic conductivity
of the medium with respect to the chemical grout or water is constant

during the injection. This is not true. The problem of chemical grout injection into a water-saturated medium is a partially saturated or multi-phase problem, and the saturation of the medium, with respect to a fluid, at a given location is changing with time. Since the hydraulic conductivity is a function of saturation then obviously the hydraulic conductivity of the medium at any point with respect to either fluid is also changing with time and is <u>not</u> a constant. Therefore, Eq. (12) is not valid for predicting Newtonian grout penetration distances because it is based on the erroneous assumption that hydraulic conductivity is constant in two-phase flow. However, for the special case where the chemical grout viscosity and density is nearly the same as water, then the conductivity is almost constant. Since many of the widely used chemical grouts have viscosities and densities very close to that of water, Eq. (12) can be used for these fluids to approximately predict penetration distances. Herndon and Lenahan (1976) report that the equation gave good results for some case histories where chemical grouts with very low viscosities and controlled gelling times were used.

In Appendix II of this report I have derived an equation similar to Eq. (12) for the case of injection from a cylindrical source resulting in a grouted mass of cylindrical shape. The length of the injection pipe is considered to equal the length of the resulting grouted cylinder. This derivation was carried out because in cases where horizontal conductivity is much greater than vertical conductivity, the grouted mass is of cylindrical shape (Karol, 1968).

The equation obtained using procedures and assumptions similar to those outlined by Herndon and Lenahan (1976) for deriving the Raffle and Greenwood equation shown above is

$$t = \frac{n}{(H_1 - H_2) \, K} \left\{ r^2 \left[\frac{\ln(r/r_0)}{2} - \frac{1}{4} \right] + \frac{r_0^2}{4} \right\} \tag{13}$$

where all symbols are the same as before, with the additional use of H_2 = in situ hydraulic head of water. This equation is similar to Raffle and Greenwood's in that for a given fluid and porous medium the radius of penetration depends on time. Again, Eq. (13) can only be used in the special case where the grout viscosity and density is nearly the same as water.

D. Discussion of Available Methods for Prediction of Penetration Distance of Particulate Grouts

The only method found during this study for predicting the maximum distance of penetration of a non-Newtonian, particulate grout with a yield strength was presented by Raffle and Greenwood (1961). They started their analysis by recognizing that it was possible to predict penetration distance in straight, circular, horizontal tubes as given by Eq. (10) and repeated here:

$$L_{max} = \frac{R \, \gamma_g (H_g - H_w)}{2 \tau_y}$$

where L_{max} = maximum penetration distance; H_g = injection pressure head; H_w = in situ pressure head; γ_g = specific weight of the grout; and τ_y = yield strength of the grout. In grouting we usually know the fluid properties γ_g and τ_y, the in situ pressure head H_w, and the maximum injection pressure head H_g possible with a given grout pump. Therefore, Raffle and Greenwood reasoned that if they could determine some value representative of the "average" or "equivalent" radii of pores in a porous medium, i.e., determine "R", then they could use Eq. (10) to predict L_{max}.

In order to determine R, which Raffle and Greenwood assumed to be characteristic of the soil, they used the Kozeny-Carman approach for theoretically determining hydraulic conductivity (see Appendix I or Mitchell (1977) for complete description). My interpretation of their method is that they implicitly assumed that a bundle of parallel tubes of radius R is hydraulically equivalent to a porous medium of conductivity K. Figure 9 shows the conceptual model where the implicit assumption is made that the area of flow in the tubes is equal to the total cross-sectional area (solids plus voids) of the porous medium multiplied by the porosity n (i.e., $A_f = A\,n$). The two mediums are hydraulically equivalent in that the flow rate Q through them is equal for the same hydraulic gradient. Thus,

$$Q = \frac{b\pi R^4 i \gamma}{8\mu} \quad \text{for the bundle (Poiseuille's Law)}$$

where b = number of tubes in the cross section such that

$$A_f = A \, n = b\pi R^2,$$

$\quad$ i = hydraulic gradient,

$\quad \gamma$ = specific weight of fluid,

$\quad \mu$ = absolute viscosity of the fluid.

Also,

$$Q = KiA \quad \text{(Darcy's Law for soil)}$$

Then,

$$\frac{b\pi R^4 u \gamma}{8\mu} = KiA$$

Substituting $b\pi R^2 = An$ we obtain

$$\frac{R^2 \gamma n}{8\mu} = K$$

thus

$$R = \sqrt{\frac{8\mu K}{\gamma n}} \tag{14}$$

which was obtained by Raffle and Greenwood. Therefore, Raffle and Greenwood believed that R was a unique characteristic of any soil and depended on K, n, γ and μ. Scott (1963) called R the "effective radius of an average pore passage" but I feel that is an incorrect description of R which is really the radius of a capillary in an idealized bundle

of tubes and is not an actual measurement of any aspect of soil geometry.

Raffle and Greenwood then use R in Eq. (10) to determine L_{max}. Although their approach was clever and ingenious I feel that it is incorrect and that their approach cannot be used to predict penetration distance for the non-Newtonian grouts. I disagree with two fundamental assumptions implicit in their solution. First, the problem is really a two-phase flow problem where the conductivity of the medium with respect to the two fluids is no longer a constant, as pointed out in the previous section. Raffle and Greenwood use results from single phase flow models and assume that these results are valid for a two-phase flow problem. This is not true. Second, I disagree with their implicit assumption that R, which is determined using Newtonian fluid flow equations, is also characteristic on non-Newtonian fluid flow. Poiseuille's Law and Darcy's Law simply do not apply to grout flow. If there is some equivalent capillary tube radius R_g for grout flow, then we should be able to determine its value using non-Newtonian fluid flow equations. Using a similar approach to that taken by Raffle and Greenwood and assuming Bingham fluid behavior, we have

$$Q = \frac{}{8\mu_B} \left[1 - \frac{4}{3}\left(\frac{2\tau_y}{R_g i \gamma_B}\right) + \frac{1}{3}\left(\frac{2\tau_y}{R_g i \gamma_B}\right)^4 \right]$$

for the bundle (Buckingham's equation), where $b = An/\pi R_g^2$ as before.

Also, using the generalized Darcy's Law proposed in the following section where the hydraulic conductivity is a function of the hydraulic

gradient, we have $Q = K_B iA$ where K_B is the hydraulic conductivity for a Bingham fluid at a given i. Then,

$$\frac{b\pi R_g^4 i \gamma_B}{8\mu_B} \left[1 - \frac{4}{3}\left(\frac{2\tau_y}{R_g i \gamma_B}\right) + \frac{1}{3}\left(\frac{2\tau_y}{R_g i \gamma_B}\right)^4 \right] = K_B iA \quad .$$

Substituting $b\pi R_g^2 = An$ we obtain

$$R_g = \sqrt{\frac{8\mu_B K_B}{n\gamma_B \left[1 - \frac{4}{3}\left(\frac{2\tau_y}{R_g i \gamma_B}\right) + \frac{1}{3}\left(\frac{2\tau_y}{R_g i \gamma_B}\right)^4 \right]}} \quad . \tag{15}$$

This equation is not nearly as simple as the one obtained for Newtonian fluid flow by Raffle and Greenwood's method. For one thing R_g can only be obtained by trial and error solution. For another, R_g is obviously a function of the hydraulic gradient, something that was not true in Raffle and Greenwood's equation. However, when we try to use R_g to find L_{max}, the maximum distance of penetration, we immediately run into a major snag. The appropriate R_g to use in Eq. (10) is determined by using the critical hydraulic gradient, i_c, in Eq. (15). The critical hydraulic gradient i_c is defined the same as the critical pressure gradient G_c in Eq. (10); that is, i_c = the non-zero hydraulic gradient below which no grout flow occurs in the porous medium.

If $Q = 0 = K_B i_c A$ and $i_c \neq 0$ and $A \neq 0$, then $K_B = 0$. Therefore, $R_g = 0$ and Eq. (10) produces the uninteresting and uninformative

result that L_{max} = 0. This same result will occur if we use Casson or Herschel-Bulkley models.

In conclusion, the Raffle-Greenwood method to determine maximum grout penetration distance does not work simply because their assumption that a characteristic hydraulically equivalent capillary tube radius based on single-phase Newtonian fluid flow also applies to a two-phase non-Newtonian flow problem is not valid. Using non-Newtonian fluid flow behavior and using a similar approach we can obtain a characteristic tube radius for grouts but this radius depends on the hydraulic gradient and as a result of K_B = 0 at i_c we get a nonsense answer. Thus, the research for a characteristic pore radius based on porous medium and fluid properties is not useful for determining the penetration distance for a grout.

E. An Analysis of the Applicability of Darcy's Law to Particulate
   Grout Flow Through a Porous Medium

If all particulate grouts had Newtonian fluid characteristics then the Buckley-Leverett equation presented in Section C could be used to predict penetration distances. As mentioned previously, most chemical grouts do have Newtonian properties and, therefore, do not present much of a problem as far as prediction of grout penetration. The fundamental relationship that describes flow of Newtonian fluids through porous media is Darcy's Law. Obviously, one approach to determining the penetration distance of particulate grouts (i.e., non-Newtonian fluids) is to use Darcy's Law much the same as Buckley and Leverett used Darcy's Law for Newtonian fluids. Thus, it is worthwhile to

examine the question "Does Darcy's Law apply to non-Newtonian fluids that have a yield strength?"

Darcy's Law for one-dimensional fluid flow in a porous medium can be simply stated as

Q = KiA

where Q = flow rate; K = hydraulic conductivity;

i = dH/dL rate of change of hydraulic head with respect to

length; and A = cross-sectional area of porous medium.

Another way of stating Darcy's Law is that (Q/A)/i = K = constant for a given fluid and porous medium at a constant percent saturation. Darcy's Law is an empirical equation where K is determined experimentally either by a standardized laboratory test or by a field test.

The following assumptions apply for Darcy's Law:

1. The fluid considered is a Newtonian fluid with constant absolute viscosity.

2. The saturation of the medium with respect to the fluid is constant.

3. The flow must be laminar. If the Reynolds number is greater than 1 to 10 then turbulent flow will result and Darcy's Law is not applicable (Freeze and Cherry, 1979).

4. Darcy's Law applies only on a macroscopic level, not a microscopic level.

5. The flow can be steady-state or transient.

6. The porous media can be homogeneous or heterogeneous and

   isotropic or anisotropic.

It is obvious from the first assumption stated above that, as it
stands, Darcy's Law cannot be applied to non-Newtonian fluid flow
without experimental or theoretical verification.

Darcy's Law leads to some important corollaries that are significant
when we examine flow of a particulate grout. One important corollary is
that Newtonian fluid flow will always occur in any porous medium with
non-zero K as long as i is greater than zero. That is, no matter how low
a hydraulic conductivity a soil has and no matter how low a hydraulic
gradient we use, as long as K > 0 and i > 0, then Q > 0, and some flow
will occur. A consequence of this phenomenon is that for grout injection
of a Newtonian fluid we can create any size grouted mass we want of radius
r as long as we maintain injection pressures for a sufficient time. This
is because the hydraulic gradient for grout injection will always be
greater than zero when the injection head is greater than the in-situ
piezometric head. Thus, the radius of penetration of a Newtonian grout
is a function of time alone as long as i and K are non-zero.

Another important corollary of Darcy's Law concerns saturation and
flow paths. For Newtonian fluids saturation is a function of fluid
availability and time; that is, if enough fluid is available and if we
allow enough time for flow to occur to the most remote pores, then the
medium will become completely saturated because, as we stated above,
flow will always occur under any non-zero hydraulic gradient. A

saturation value of 100 percent is a common occurrence in nature. This also means that all voids, no matter how small, are potential flow paths as long as they are somehow connected to other voids. With regard to grouting, this means that all voids can be filled with a Newtonian grout if we maintain injection pressures for a sufficient time.

A third corollary concerns the definition of intrinsic or specific permeability which is

$$k = \frac{K\mu}{\gamma} \tag{16}$$

where k = intrinsic permeability;

$\quad$ K = hydraulic conductivity,

$\quad$ μ = absolute viscosity of permeant, and

$\quad$ γ = specific weight of permeant.

Experiments with ideal and real porous media have shown that the intrinsic permeability depends only on porous media properties as long as the permeant is a Newtonian fluid.

Darcy's Law is an empirically derived description of fluid flow. A theoretically derived equation for the hydraulic conductivity has been obtained and is known as the Kozeny-Carman equation (Mitchell, 1976), where

$$K_N = \frac{\gamma_N e^3 S^3}{\mu_N C_0 TS_0^2 (1 + e)} \tag{17}$$

where K_N = hydraulic conductivity for Newtonian fluid,

S_0 = specific wetted surface area of grains per unit volume,

e = void radio,

C_0 = pore shape factor (dimensionless),

T = tortuosity factor (dimensionless),

γ_N = specific weight of Newtonian fluid,

μ_N = absolute viscosity of fluid,

S = saturation.

The derivation of this equation for porous media is based on an analogy with the flow of a fluid in a straight capillary. The basic assumption is that the porous medium consists of a series of flow channels or capillaries where resistance to flow depends on a properly defined hydraulic radius (Duncan et al., 1972). This formula can be used to predict hydraulic conductivity for uniformly graded sands and silts but does not work for clays due to the effect of a wide range in pore sizes (Mitchel, 1976).

The main use of the Kozeny-Carman equation is to give a conceptual understanding of fluid flow phenomena. In the first place we see that hydraulic conductivity fundamentally depends on fluid properties--γ_N, μ_N, S--and media properties--e, S_0, C_0, T. Second, we see that the most important parameters are those which are measures of pore size--e, S_0. Third, we see that the intrinsic permeability based on the Kozeny-Carman equation is only a function of the geometric properties of the medium. Therefore, the Kozeny-Carman equation theoretically confirms our understanding of the empirically based Darcy's Law.

In order to gain an understanding of the fundamentals of flow of non-Newtonian grout in a porous medium, an approach similar to the Kozeny-Carman approach for Newtonian fluids described above was used. Detailed derivations of Kozeny-Carman type equations of Bingham, Casson, and Herschel-Bulkley fluids are given in Appendix I. As was discussed in Section A, the essential difference between Newtonian and non-Newtonian fluid flow in capillaries is that non-Newtonian fluids with a yield strength develop an unsheared cylinder in the center of the capillary (see Fig. 4).

Following is a list of the Kozeny-Carman type equations that express the hydraulic conductivity of the fluid in a given porous medium:

Newtonian fluid

$$K_N = \frac{\gamma_N e^3 S^3}{\mu_N C_o T\, S_o^2 (1 + e)}$$

Bingham fluid

$$K_B = \frac{e^3 S^3 \gamma_B}{\mu_B C_o T S_o^2 (1 + e)} \left[1 - \frac{4}{3}\left(\frac{S_o \tau_y}{eSi\gamma_B}\right) + \frac{1}{3}\left(\frac{\tau_y S_o}{eSi\gamma_B}\right)^4 \right] \tag{18}$$

Casson fluid

$$K_C = \frac{e^2 S^2}{\mu_C C_o T S_o i (1 + e)} \left[\frac{eSi\gamma_C}{S_o} - \frac{4}{7}\left(\frac{eSi\gamma_C \tau_y}{S_o}\right)^{1/2} + \frac{\tau_y}{3} - \frac{\tau_y^4 S_o^3}{84(eSi\gamma_C)^3} \right] \tag{19}$$

Herschel-Bulkley fluid

$$K_{H-B} = \frac{S(eS_i\gamma - S_o\tau_y)^{m+1}}{C_oT(eS)^2 i^4 \gamma^3 \mu^m S^{m-1}(1 + e)} \left[\frac{(eSi\gamma - S_o\tau_y)^2}{S_o^2(m + 3)} \right.$$

$$\left. + \frac{2\tau_y(eSi\gamma - S_o\tau_y)}{S_o(m + 2)} + \frac{\tau_y^2}{m + 1} \right] \qquad (20)$$

Comparing these equations with the equation for Newtonian fluids, several important conclusions can be reached. First, obviously the relationships become much more complex. Second, if we try to determine the intrinsic permeability as was done for Newtonian fluids, we see that it is impossible to get a similar relation which is independent of fluid properties. Thus, the notion of intrinsic permeability which depends only on porous media properties does not apply to non-Newtonian fluid flow. Third, and most importantly, we see that in every case the theoretical value of hydraulic conductivity, K, is a complex function of the hydraulic gradient, i, whereas for a Newtonian fluid K is theoretically independent of i. The reason that K is a function of i for the non-Newtonian fluids appears to be due solely to the yield strength, τ_y, of the fluid. For the Bingham fluid we see that if $\tau_y = 0$ then K is no longer a function of i. However, for the Herschel-Bulkley and Casson fluids K is still a function of i if $\tau_y = 0$ and $m \simeq 1$. Therefore, based on a Kozeny-Carman analysis, the hydraulic conductivity K of a porous medium with respect to a non-

Newtonian particulate grout is not a constant and, consequently, Darcy's Law does not apply to particulate grout flow.

In addition to the theoretical analysis presented above, experimental evidence regarding particulate grout flow in a porous medium is available. Marsland and Loudon (1963) carried out a series of conventional conductivity tests on a uniformly graded river sand using a bentonite grout which behaved approximately as a Bingham fluid. Figure 10 shows the generalized results of their tests. The curve for the bentonite slurry is similar to that for a Newtonian fluid except that there is a non-zero intercept i_c on the hydraulic gradient axis. By definition i_c is called the critical hydraulic gradient. If the hydraulic gradient is less than i_c, then flow ceases. Also for gradients such that $i_c < i < i_b$ the slope of the curve is not a constant, i.e., $K_B \neq$ constant. These results verify the Kozeny-Carman type relationship given by Eq. (18) since as $i \to \infty$ then $K_B \to$ constant. A physical interpretation of Marsland and London's results is that as the gradient through the test apparatus is decreased the size of the unsheared cylinder of grout referred to in Fig. 4 is increasing. When the radius of the unsheared cylinder is equal to the radius of the pores in the sand sample, flow ceases. Therefore, the critical hydraulic gradient i_c must be related to the pore radii and the yield strength of the grout.

In conclusion, the Kozeny-Carman analysis and experimental evidence indicate that flow of a non-Newtonian grout through a porous medium is fundamentally different than flow of a Newtonian fluid. Darcy's Law

does not apply to particulate grout flow simply because the grouts
cause an unsheared cylinder to form within the flowing mass. When the
diameter of this unsheared cylinder is equal to the pore diameter of
the soil then flow ceases. However, a Darcian-type relationship for a
particulate grout flow is suggested by the above considerations. That
is, for non-Newtonian fluids flowing in a porous medium we have this
constitutive equation:

$$Q = K(i) \ i \ A \tag{21}$$

where $K(i)$ signifies that the hydraulic conductivity is not a constant
but is a complex function of the hydraulic gradient as well as of the
media and fluid properties. Although it may be possible to use
Eq. (21) to predict the penetration distance of particulate grouts, I
will not pursue that course. The reason for this is that I suspect
that approach may lead to differential equations that will be very
difficult to solve either analytically or numerically. Also, as will
be shown in the following section, I think a much simpler approach
leading to a simple linear model is possible.

F. Proposed Equation for Predicting Penetration Distance of a
Particulate Grout in a Porous Medium

As mentioned in the previous section, Darcy's Law cannot be used
to solve the problem of predicting penetration distances of particulate
grouts. A generalized Darcian-type law could probably be developed
for non-Newtonian fluids but could lead to differential equations that
are very difficult to solve either analytically or numerically.

Instead I have decided to approach the problem from a phenomenological viewpoint. This will result in an empirical equation that contains experimentally determined coefficients. This type of approach is commonly used in fluid mechanics, especially in hydrodynamics, because of the difficulties in theoretically characterizing turbulent, non-uniform flow.

In Section B, Eq.(10) was derived. This equation allows one to theoretically predict the maximum penetration distance of a non-Newtonian fluid with a yield strength in a straight, circular, horizontal tube. This equation can be presented as

$$L_{max} = \frac{R(P_i - P_0)}{2\tau_y} \tag{22}$$

where L_{max} = distance from tube inlet to grout front when flow ceases; R = radius of tube; P_i = pressure at inlet, i.e., injection pressure; P_0 = hydrostatic pressure of Newtonian fluid in tube before injection begins and when flow stops, i.e., in situ fluid pressure; and τ_y = yield strength of the non-Newtonian fluid. However, this equation can not be used for a porous medium because pore passages are not straight, not circular, and do not have a constant radius along their length. I propose to modify Eq. (22) so that it can be used for porous media. In order to do this I will add coefficients that will correct for non-circularity, sinuosity, and varying radius of the pore passages in a porous media. But, one fundamental assumption must be made, that is, when a non-Newtonian fluid flows along a porous passage

an unsheared cylinder forms in the center of flow as shown in Fig. 4. When the radius of this cylinder is as large as the "radius" of the pores then flow will cease. In other words, the yield strength of the fluid, τ_y, will develop a frictional shear force along the walls of pores that will effectively resist the positive pressure forces created during injection and cause flow to stop. When flow ceases the problem reduces to a fluid statics condition and is much easier to handle because τ_y, P_i, and P_0 are usually known for a particular case.

The first coefficient that will be added is the Tortuosity Factor--T. The tortuosity factor will correct for the sinuous nature of the pore passages in a porous medium. Figure 11 shows schematically the effect of sinuosity on the maximum distance of penetration and how tortuosity is defined. The resisting shear force developed by the grout depends on the length of contact--L_c--of the grout with the pore wall. But the radius of the grouted mass about the injection pipe--L_{max}--is measured as the shortest distance between the pipe and grout front and is obviously less than L_c. The tortuosity factor is the average ratio of the actual length of contact to the shortest horizontal length, L_s, between a point in the pore passage and pipe for all points along the pore, that is, $T = L_c/L_s$. This dimensionless coefficient is a geometric property of the porous medium and should not depend on grout properties or injection pressures. The tortuosity factor was also used in the Kozeny-Carman theoretical determination of the hydraulic conductivity (see Eq. (17)). Carman (1937) observed from his tests using an ideal porous medium made of glass spheres and tests

using real porous media that T was generally between 1.2 and 1.6. In practical applications a value of 1.4 is a good approximation for T (Duncan, et al., 1972).

The second coefficient that should be added is the Pore Shape Factor--C. The pore shape factor will correct for the non-circular nature of pore passage cross-sections. Figure 12 schematically illustrates a non-circular pore shape that can be found in media and how the unsheared cylinder in the center of flow must change shape as it increases in size with decreasing pressure gradient. If the un-sheared zone is the same size and shape as the non-circular pore then flow of grout will cease as pointed out before. The pore shape factor is also a property of the porous medium and should be independent of the grout properties and injection pressures except for the case where pressures are so high that the structure of the porous media is changed. C can be defined as the ratio between L_{max} in a non-circular tube to L_{max} in a circular tube of the same hydraulic radius and for the same grout. I would suspect that pore shapes in a modified in situ retort are generally rectangular or triangular.

The problem of non-circularity of the pore passages must also be handled by using the hydraulic radius, R_H, for the cross-sectional dimension. By convention, the hydraulic radius is defined as

$$R_H = \frac{\text{Area}}{\text{Wetted Perimeter}} \qquad (23)$$

For a circular tube

$$R_H = \frac{\pi R^2}{2\pi R} = \frac{R}{2} \quad .$$

Therefore, for a sinuous, horizontal, non-circular tube of constant hydraulic radius Eq. (22) becomes

$$L_{max} = \frac{R_H \; C \; (P_i - P_o)}{T \cdot \tau_y} \tag{24}$$

However, Eq. (24) can only be used in tubes of constant hydraulic radius along their length. Pore passages in a porous medium do not have constant hydraulic radius. Thus, the varying hydraulic radius requires that Eq. (24) be used in an iterative fashion in order to determine the maximum penetration distance. Figure 13 illustrates a pore passage with varying hydraulic radius where the radius and length of each section are known, that is R_{Hx} and L_x are known. Also, the yield strength of the grout τ_y, the injection pressure P_i, the in situ pressure P_o, and the pore shape factor C are known. For the first part of analysis we neglect the Tortuosity Factor T. In order to find L_{max} we guess at values of L_{max} and then use the concept of the critical pressure gradient illustrated in Fig. 4 where the

$$\text{critical pressure gradient} = G_c = \frac{C \; \tau_y}{R_H} \tag{25}$$

for non-circular pore shapes. If our guess for L_{max} is correct we stop, if not, we make another guess and repeat our critical pressure gradient calculation. An important point to recognize is that if the critical pressure gradient is reached across any section of constant hydraulic radius then a critical pressure gradient is reached across all sections because once the flow ceases in one section is must cease in all sections along the pore passage. The following algorithim illustrates the procedure for determining L_{max} (refer to Fig. 13):

1. Assume $L_1 = L_{max}$. Then

$$G_{c1} = G_1 = \frac{C_1 \tau_y}{R_{H1}} = \frac{P_1 - P_2}{L_1}$$

or

$$P_1 = \frac{L_1 C_1 \tau_y}{R_{H1}} + P_2$$

Since $P_2 = P_0$ when flow slops we can calculate P_1 and compare it to P_i

    (a) If $P_1 = P_i$, then $L_{max} = L_1$ and we have our answer.

    (b) If $P_1 < P_i$, then $L_{max} \neq L_1$ and furthermore we see that $L_{max} < L_1$. We then try values of $L_{max} < L_1$ in order to find a value of L_{max} that gives $P_1 = P_i$.

    (c) If $P_1 > P_i$ then again $L_{max} \neq L_1$ and furthermore we see that $L_{max} > L_1$. Now we estimate a value of $L_{max} > L_1$ in order to find a value that gives $P_1 = P_i$.

2. Since cases 1(a) and 1(b) above are easy to handle let us continue the solution by examining case 1(c). Assume $L_1 + L_2 = L_{max}$. Then,

$$G_2 = G_{c2} = \frac{C_2 \tau_y}{R_{H2}} = \frac{P_2 - P_3}{L_2}$$

or

$$P_2 = \frac{C_2 \tau_y L_2}{R_{H2}} + P_3$$

Since $P_3 = P_0$ when flow stops we can calculate P_2 which in turn allows us to calculate $G_{c1} = G_1$, because as stated above, when the critical pressure gradient is reached in one section, it is simultaneously reached in all the preceding sections of the pore passage. Therefore,

$$G_1 = \frac{C_1 \tau_y}{R_{H1}} = \frac{P_1 - P_2}{L_1}$$

and

$$P_1 = \frac{L_1 C_1 \tau_y}{R_{H1}} + P_2$$

We compare P_1 to P_i as before.

(a) If $P_1 = P_i$ then $L_{max} = L_1 + L_2$.

(b) If $P_1 < P_i$ then $L_1 < L_{max} < L_2$ and we iterate again using a value between L_1 and L_2.

(c) If $P_1 < P_i$ then $L_{max} < L_1 + L_2$ and we iterate again using a value greater then $L_1 + L_2$, say L_3.

(3) The above steps are repated as often as necessary until we estimate a value of L_{max} that yields $P_1 = P_i$. In the general case we estimate

$$L_{max} = L_1 + L_2 + \ldots + L_x$$

which yields

$$G_x = G_{cx} = \frac{C_x \tau_y}{R_{Hx}} = \frac{P_x - P_{x+1}}{L_x}$$

Then

$$P_x = \frac{L_x C_x \tau_y}{R_{Hx}} + P_{x+1}$$

where $P_{x+1} = P_0$. Once P_x is determined we can calculate P_{x-1}, P_{x-2}, . . ., P_2, P_1. Then P_1 is compared to P_i and the result of the comparison indicates the next step. Once we have an L_{max} that yields $P_1 = P_i$ we correct for tortuosity by dividing the L_{max} by T to get the actual penetration distance from the injection point.

Although this iterative solution scheme would be very tedious to carry out by hand, it can be very easily done on a computer or even a programmable calculator.

Another characteristic of pore passages in a porous medium is that the passages branch and rejoin throughout the mass. That is, pore passages are not single tubes isolated from adjoining tubes but instead form a network analogous to blood vessels in the body or a municipal water system. Therefore, grout as it is injected, has a large number of

potential paths to follow. However, because the pressure gradient in the grout is constantly decreasing as the grout front moves away from the injection point (see Fig. 7), the radius of the unsheared cylinder must be constantly increasing. This means that as the grout moves through the network the grout can only enter pore passages where the hydraulic radii of the pores are greater than the radius of the unsheared cylinder in the grout. Thus, a minimum pore radius of penetration—R_{min}—exists throughout the porous network, that is, at any given point in the network and with given conditions of injection pressure, in situ pressure and yield strength of grout, only pores with hydraulic radius greater than R_{min} can be penetrated. The value of R_{min} at any point is determined by solving Eq. (25) where

$$R_{min} \text{ at point } x = C_x \tau_y / G_{cx} \qquad (26)$$

with G_{cx} = the critical pressure gradient at x. Obviously, since G_{cx} decreases with distance from the injection point, R_{min} must increase continuously (Fig. 14a). When R_{min} is greater than R_H in any pore passage, flow ceases along that passage. Flow may continue along some tributary of that passage but eventually R_{min} will be greater than the hydraulic radius of all connecting pore passages in the network and flow of grout will cease. Since we know that flow will eventually cease throughout the porous network, we can still use the iterative analysis explained in the preceding paragraph for a branching network of pore passages. This is because when flow ceases, the critical pressure

gradient--G_c--must exist in the grout in every section of every filled pore passage in the network.

In conclusion, I propose that Eq. (24) can be used to predict the maximum penetration distance of a non-Newtonian particulate grout with a yield strength in a porous medium. Equation (24) is repeated here:

$$L_{max} = \frac{R_H C(P_i - P_o)}{T \tau_y} \qquad (24)$$

This equation must be used in an iterative fashion in order to find L_{max} for pore passages of varying hydraulic radius. This method requires that the dimensions of the pore passages, the injection and in situ pressures, the yield strength of the grout, and two coefficients characteristic of the porous medium--C and T--must be known. Also, the equation only applies to an isothermal, incompressible, non-thixotropic fluid in horizontal, two-dimensional laminar flow. The porous medium is assumed to be incompressible. In addition, the grout and the fluid initially occupying the pores--water or air are the most likely--are assumed to be immiscible, with the grout completely displacing the other fluid in the pore passages as grout is injected.

G. Consequences and Shortcomings of the Hypothesis

In the previous section a formula was proposed that predicts the penetration distance of a particulate grout given porous media properties, fluid properties, injection pressures, and initial in situ pore pressures. Several important consequences result from consideration of the hypothesis.

First, there is a fundamental difference in approach to examining flow through a porous media implied by Eq. (24). Traditionally, flow of Newtonian fluids through porous media as characterized by Darcy's Law assumes that the media is a continuum. Thus, it is not necessary to know anything about pore sizes to apply Darcy's Law since the hydraulic conductivity value--K--provides a coefficient that integrates and includes all the necessary porous media properties. Darcy's Law is appropriate for Newtonian fluids when we are concerned with macroscopic flow, that is, flow through a volume containing many pore passages. However, Darcy's Law does not provide accurate results when applied to a single flow path, and as pointed out in Section E, Darcy's Law does not apply to non-Newtonian flow. As a result, rather than adopt a continuum model of a porous media, I have suggested that for the problem at hand it is necessary to model porous media as many sinuous, interconnected tubes of non-circular shape and varying hydraulic radius. Therefore, in order to apply Eq. (24) it is necessary to have a lot more information about pore passage geometry than was required for Darcy's Law.

Second, Eq. (24) indicates the parameters that control groutability. For a given set of pressure conditions groutability appears to depend on pore passage geometry and the yield strength of the grout. However, grouts are not fluid continua but are mixtures of solids and a Newtonian fluid. Thus, we should consider the possibility that pore penetration can be prevented by particles physically blocking pores simply due to their shape and size. Many discussions in the

literature state that groutability is a function of likelihood of particle blockage and give groutability indices that are ratios between the size of particles in a grout and the size of pores (Mitchell, 1970). Obviously, if a grout containing large particles is injected into a medium containing small pores then pore blockage can occur. A common rule-of-thumb for particulate grouts is that the pore radius must be at least three times the grout particle radius in order to obtain a low probability for pore blockage (Herndon and Lenahan, 1976). But, even if all grout particles were much smaller than the soil pores, grout flow would eventually cease when the critical pressure gradient, which depends on pore geometry and τ_y is reached. In fact, Thomas (1961 and 1963) suggests that for some materials τ_y is inversely proportional to the square of the particle diameter, i.e., τ_y increases as the particle diameter decreases. This means that distance of grout penetration would decrease as the size of the particles decreases for a given volume fraction of solids to liquids. Experimental results presented in the second half of this report show that even if the ratio of grout particle size to pore size is as little as 0.0004 flow will still cease due to the resisting force created by the yield strength of the grout. Thus, groutability is not generally a function of particle blockage or ratios between pore dimension and grout particle size but is instead a function of τ_y and pore geometry.

Some other consequences of Eq. (24) concern the variation of saturation with respect to grout and the variation of hydraulic conductivity of the grouted mass with respect to water with distance from

the injection point. When we consider saturation, it can be seen that the schematic relationship shown in Fig. 14b should hold, that is, the saturation of the medium with respect to a particulate grout should decrease with distance from the injection point. This follows from the fact that larger and larger pores remain unfilled as we move away from the injection point. This variation in saturation with distance from the source is very different from what occurs for Newtonian fluids where complete saturation can occur as long as fluid is available and injection pressures are maintained for sufficient time. With a fluid possessing τ_y it does not matter how much fluid is available or how long we maintain injection pressures, we still can not fill pores smaller than R_{min} and, consequently, 100 percent saturation is not possible in a medium with a wide range in pore sizes at the outer sections of the injected mass. Therefore, saturation is a function of G and τ_y. Because of this variation in grout saturation with distance from the injection point, there is an increase in the value of the hydraulic conductivity of the grouted mass with respect to water over the same distance as shown schematically in Fig. 14c. Therefore, the "effective" hydraulic conductivity of a grouted modified in situ retort will be the conductivity of the outer edges of the individual grouted cylinders. Consequently, in order to reduce the conductivity of the retorts the grouted cylinders should overlap so as to fill pores left unfilled on the outer edge of the initial grouted mass. Figure 15 is a section through a grouted mass that shows how the grout

actually permeates the pores and gives the relationships shown in Fig. 14.

Examination of Eq. (24) reveals two major shortcomings. The first is that the pore shape coefficient, C, must be determined by extensive testing under controlled conditions. Hundreds of tests using tubes of different cross-sectional shape are required in order to establish statistically significant values for C. The tortuosity coefficient, T, does not require extensive testing since values have already been determined by Carman (1937).

The second shortcoming is that Eq. (24) requires detailed knowledge of pore passage geometry in a porous medium. As has been mentioned previously, the key to predicting grout penetration distance lies in being able to determine the character of the flow paths. It is necessary to know how the pore hydraulic radius varies along the flow path as well as the cross-sectional shape of the pores so that the capillary flow model hypothesized here can be used. The pore size distribution can be obtained by direct measurement or by forced intrusion of a non-wetting fluid (Mitchell, 1976). Direct measurement is carried out on soilds that have been cemented by a transparent plastic or resin. Thin sections or polished surfaces are then cut and pores are measured. Three-dimensional analysis requires the measurement of several parallel sections. The forced intrusion method is based on the principle that the pressure required to inject a non-wetting fluid into a pore is inversely proportional to the pore diameter and directly proportional to

the surface tension of the fluid. Mercury is usually used for this test and apparatus for porosimetry measurements is commercially available. However, for unconsolidated materials with very large pores such as in situ retorts this method would not be very practical. Direct measurement of pores for oil shale retorts is probably the most practical method for determining pore size distribution. However, it must be realized that the above tests are not easy to carry out and are not routinely done.

In the next section of this report results of tests carried out at LBL for the purpose of verifying Eq. (24) and for determining pore shape coefficients are presented.

III. EXPERIMENTAL EVALUATION OF THE PROPOSED HYPOTHESIS FOR
      PREDICTION OF PENETRATION DISTANCE IN A POROUS MEDIUM

A. Purpose of the Experiments

In the previous section an equation was developed for providing a

prediction of the penetration distance of a particulate, non-Newtonian

grout in a porous medium. The equation is as follows:

$$L_{max} = \frac{R_H C(P_i - P_o)}{T \tau_y} \qquad (24)$$

where L_{max} = maximum distance of penetration of grout from injection

            point,

  R_H = hydraulic radius of the pore,

  P_i = injection pressure,

  P_o = pore pressure before injection begins,

  τ_y = yield strength of the grout,

  C = pore shape factor,

  T = tortuosity factor.

The assumptions applicable to the equation are that the fluid is

incompressible and non-thixotropic, and the flow is isothermal, hori-

zontal, two-dimensional, and laminar. In addition, the grout is

assumed to be immiscible with the fluid being displaced (i.e., either

air or water). In order to test this equation a series of experiments

was carried out during the period August 1980-June 1981.

The purpose of the experiments was to determine if the proposed

equation was valid for straight, circular tubes of constant hydraulic

radius. In this case, $C = 1$, $T = 1$, and $R_H = R/2 =$ hydraulic radius of the tube which yields

$$L_{max} = R(P_i - P_o)/2\tau_y \qquad \qquad (27)$$

By comparing actual penetration distances to predicted distances, the validity of Eq. (27) would be established. Following the tests on circular tubes, penetration tests using straight, non-circular tubes of constant hydraulic radius were carried out. The ratio of the penetration distance in a non-circular tube to the penetration distance of the same grout in a circular tube of the same hydraulic radius as the non-circular tube would yield the pore shape factor, C. A total of 15 circular tube and 25 non-circular tube penentration tests were carried out. The results of the individual tests are given in Table 3. Time did not permit tests using ideal porous media constructed of solid glass spheres or of real porous media such as tubes filled with spent shale. Further testing should be carried out using both ideal and real porous media.

B. Experimental Set-Up

The experimental set-up and apparatus are shown schematically in Fig. 16. The apparatus consisted of four parts--pressure tank, injection tube, pressure transducer, and bentonite slurry.

1. Pressure Tank

The pressure tank is a 6 in. diameter brass cylinder, 12 in. long. The tank was designed by Peter Persoff and manufactured at the LBL machine shop. Plate 1 is a view of the tank (the wooden rule is

15 in. long). The tank acts as a reservoir for the bentonite slurry during the penetration tests and injection pressure for the tests is supplied in the tank. The tank is pressurized from a 200 s.c.f. compressed air cylinder. A rotor or paddle extends into the tank and is turned by a small electric motor at 300 rpm. The rotor is used to stir the grout at a constant rate so as to insure uniform mixing and to reduce thixotropy in the bentonite slurry used in the tests. A pressure gage is attached to the top of the tank. A sliding gate valve is used to control flow from the outlet at the bottom of the tank. The tubing was 3/4 in. diameter flexible PVC with brass fittings connecting the tank to the injection tube. A 3/4 in. PVC ball valve controls flow from the pressure tank into the injection tube.

2. Injection Tubes

Ten injection tubes with different cross-sectional shapes and hydraulic radii were used in the penetration tests: three circlar, two triangular, two rectangular, and three star-shaped. The circular and star-shaped tubes were Lucite. The triangular and rectangular tubes were composed of a combination of Lucite and aluminum. Figure 17 shows typical cross-sections of the various tubes used. Figure 18 illustrates how the tubes were machined so as to fit the 3/4 in. ball valve at the bottom and the 1/4 in. pressure measuring port was attached. Tube length was 2 m for the circular, triangular, and rectangular tubes, and 1.5 m for the star shaped tubes. Plate 2 illustrates how the penetration distance was measured. The tubes were mounted vertically on a steel rack in order to obtain complete filling

48

of the tube during injection. Also a vertical setup allowed the use

of relatively short tubes for the low pressures (1 to 6 psi) utilized

in the tests. Use of a vertical setup meant that a gravitational force

must be included in Eq. (24). This is discussed in Section D. Only

air-filled, dry tubes were used during the tests. This meant that the

P_o term in Eq. (24) was zero.

3. Pressure Transducer

Because non-Newtonian fluids will stop flowing at a non-zero

pressure gradient, it is not possible to measure pressures in a

particulate grout with a piezometer or manometer. Since low pressures

had to be used in the penetration tests in order to have reasonably

short tubes, an electrical pressure transducer was used for pressure

measurement. Plate 3 shows the pressure transducer (the white object

in the center of the photo) and its attachment to the pressure measur-

ing port in the injection tube. Plate 4 shows the x-y plotter that

was attached to the transducer and provided a plot of pressure change

versus time during the test. A Data Instrument Inc. Model AB-6 General

Purpose Transducer with a 0-6 psig range and 1 percent accuracy was

used. The transducer was connected to the 1/4 in. I.D. pressure

measuring port by a 1/4 in. I.D. PVC tube filled with water. Since

the water is nearly incompressible, the pressure of the   slurry

at the measuring port would be transferred to the transducer without

any flow of the slurry into the water-filled PVC tube connecting the

port to the transducer. Plate 5 shows the entire setup in the lab.

4. Particulate Grout

Several particulate slurries were tested using a Contraves Rheomat 15T rotational viscometer in order to determine their fluid properties. The results of the viscometer tests are given in Table 2. Figure 19 is the flow curve for one of the slurries used in several tests. For the penetration tests, a slurry of distilled water and bentonite with a water-solid ratio of 6.7:1 was used. A lignin sulfonate dispersant was added in varying amounts in order to vary the yield strength of the slurry and to reduce thixotropy. Distilled water was used for the tests with a temperature of 18.5 to 20.5°C. Cement grade ("Big Horn") bentonite, 99 percent less than 200 mesh, supplied be Wyo-Ben Inc. and lignin sulfonate dispersant, product No. CZ-512L, supplied by Crown Zellerbach Chemical Products Division was used. The grout was pre-pared by mixing, at 1300 rpm, the water, bentonite, and dispersant for 15 min with a Jiffy Mixer attached to an electric drill.

C. PENETRATION TEST PROCEDURE

Test procedure was as follows:

Step 1. The grout was poured into the pressure tank, about 4 to 5 liters. The grout was then stirred at 300 rpm by the rotor for the duration of the test. Injection was not begun until the grout had been stirred for at least 10 min in the tank.

Step 2. The pressure transducer was calibrated by attaching it to a spare injection tube and filling the tube to known heights with water. The pressure head of water on the transducer was corrected for temperature. This calibration procedure was carried out every test

Table 2. Results of rotational viscometer tests on various grout mixer.

Materials	Water-Solid Ratio	Dispersant as Percent of Solids (Percent)	Yield Strength τ_y - dyne/cm^2	Remarks
Portland Cement (Type I)	10:1	0	0	Cement particles settled out
Portland Cement (Type III)	1:2	0	92-165	Very thixotropic
	1:2.5	0	50-350	
	3:8	0	?	Extremely rheopeotic
Bentonite (Dak Southern)	5:3	0.7	380	Slightly thixotropic
	5:3	0	639-840	Very thixotropic
	2:1	0.4	191-223	Slightly thixotropic
	2:1	4.0	263-350	Slightly thixotropic
Bentonite (Wyo-Ben)	6.7:1	7.5	340-360	Slightly thixotropic
	10:1	10.0	35	Slightly thixotropic
	6.7:1	26.0	165-196	Slightly thixotropic
	8:1	16.0	65-80	Slightly thixotropic
	6.7:1	17.0	190-215	Slightly thixotropic
	6.7:1	10.0	460-560	Slightly thixotropic

because of the sensitivity of the transducer to changes in atmospheric pressure. After calibration the transducer was connected to the pressure measuring port as shown in Plate 3. The hydraulic radius, R_H, of the injection tube was recorded.

Step 3. Pressure would be applied at the tank at some arbitrary value as measured on the tank gage. The ball valve at the bottom of the injection tube would then be opened causing grout to flow up into the tube.

Step 4. When the grout-air interface in the injection tube stopped moving and pressure, P_i, at the transducer was constant, the penetration distance, L_{max}, from the measuring port to the grout-air interface was recorded. This is shown in Plate 2. It usually took 2 to 4 hr for the interface to cease moving.

Step 5. The pressure at the tank would be shut off and the ball valve removed from the bottom of the injection tube. The grout in the tube was collected and tested in the viscometer. The value of the yield strength, τ_y, of the grout injected was then recorded. As a result, all the parameters for Eq. (24) were available keeping in mind that the in situ pore pressure, P_o, was zero for air-filled, open tubes.

The apparatus used and the procedure followed appeared to yield reliable, reproducible data. There were no problems encountered in operating the equipment. The penetration tests were carried out during the period January to May, 1981.

D. Results and Analysis of Experimental Data

Table 3 contains the results of the vertical penetration tests which were carried out as described in the previous section of this report. Since the penetration tests were done in vertical tubes rather than horizontal tubes, it is necessary to modify Eq. (24) in order to include gravitational forces. Referring to Fig. 20, which shows the forces and pressures acting on a circular, vertical column of grout of constant radius where flow of grout from the bottom to the top has ceased, we have the following force balance:

$$P_i \pi R^2 = P_o \pi R^2 + \tau_y 2\pi R L_{max} + \gamma_g \pi R^2 L_{max} \tag{28}$$

or

$$(P_i - P_o) R = L_{max}(2\tau_y + \gamma_g R)$$

Thus,

$$L_{max} = \frac{(P_i - P_o) R}{2\tau_y + \gamma_g R} \tag{29}$$

Therefore, Eq. (29) takes into account gravitational forces for a vertical, circular column and replaces Eq. (27) for the vertical penetration tests. Similarly, for non-circular, sinuous tubes of constant hydraulic radius Eq. (29) becomes

$$L_{max} = \frac{C(P_i - P_o) R_H}{T(\tau_y + \gamma_g R_H)} \tag{30}$$

where C = pore shape factor and T = tortuosity factor. Likewise,
Eq. (30) replaces Eq. (24) for the vertical penetration tests carried
out at LBL.

Since the grouts used in the tests all had the same specific weight
(γ_g = 1060 dynes/cm^3) and the tests were done in air-filled open tubes
where P_o = 0, we can assume that γ_g and P_o in Eqs. (29) and (30) are
constants. This simplifies the analysis because we then see that
the distance of penetration is a function of three parameters for a
tube of given cross-sectional shape and tortuosity, that is, L_{max} =
$f(P_i, R_H, \tau_y)$. Therefore, using the concepts of dimensional analysis
we should find that our data falls on a line on a plot of L_{max}/R_H
versus P_i/τ_y.

For the tests carried out at LBL, both circular and non-circular,
straight, vertical tubes were used. Therefore, data for circular tubes
should fall on the same line on a dimensionless plot and data for the
non-circular tubes should fall on different lines because of vari-
ation in the pore shape factor, C (T = 1 for all tests since the
tubes are straight). However, data for tubes of a given shape should
fall on the same line even though there dimensions may be different.
Figures 21-24 are the dimensionless plots for the circular, triangular,
rectangular, and star-shaped tubes respectively.

Examination of Fig. 21 reveals that there is no correlation between
the variables used, for grout injection into circular tubes! This
means that Eq. (29) is not valid and that my hypothesis for predicting
grout penetration distances is not verified. Similarly, examination

of the first part of Table 2 shows that grout penetration distances predicted by Eq. (29) for circular tubes are not the same as the actual distances measured except for test 2. However, examination of Figs. 22-24 indicates that data for the non-circular tests does fall on a line and provides excellent correlation between the variables. Thus, the data for non-circular tubes verifies Eq. (30) and appears to verify my hypothesis! Obviously, there is a contradiction somewhere. It should be pointed out that the same grout batch was used for the non-circular tests but different grout batches were used for some of the circular tests, that is, the water-bentonite ratio was the same but different amounts and kinds of dispersants were used in the different batches. Theoretically, this should make no difference in the dimensional analysis but may be significant as will be discussed in detail below.

When a dimensional analysis indicates no correlation between variables, as is suggested by examination of Fig. 21, three possible reasons are indicated:

1. It may be that not all the variables necessary to describe the phenomenon have been identified and included in the analysis. But Figs. 3 and 20, which show the free-body diagram and statics analysis of the grout element, seem to contain all the relevant parameters. There just do not seem to be any other forces acting on the element. Therefore, all the variables necessary for dimensional analysis seem to have been included.

2. Another possibility is that one of the independent variables used in the analysis is not independent but in fact is dependent on other variables. For example, in this analysis L_{max} is dependent on R_H, P_i, and τ_y which were assumed to be independent variables. However, it may be that one of R_H, P_i, or τ_y may be dependent on one of the other independent variables.

3. Finally, it is possible that one of the variables has been incorrectly measured. Examination of the experiment procedures indicates that measurement of L_{max}, R_H, P_i, γ_g, and P_o is straightforward and present no difficulties. However, measurement of τ_y is not so simple. Therefore, τ_y will be more closely examined in the following paragraphs.

When the hypothesized equation for predicting the penetration distance was developed in Section I-B, it was explicitly assumed that the shear stress developed at the a wall of a tube, τ_w, when flow of a non-Newtonian fluid ceased was equal to the yield strength of the fluid, τ_y, as determined in a viscometer. This assumption is implicit in the work of other researchers in non-Newtonian fluid flow such as Wilkinson (1966), Skelland (1967), Hughes (1979), and Raffle and Greenwood (1961). As Fig. 1 illustrates, τ_y was the shear stress below which no flow occurs. It is possible to determine τ_w in the circular tube experiments by manipulating Eq. (30) as follows:

$$\tau_w = \frac{R(P_i - P_o - \gamma_g L_{max})}{2 L_{max}}$$

(31)

This value of τ_w is the average shear stress at the tube wall and is given in Table 2 for the straight circular tubes. Except for test No. 2, all the penetration tests show that $\tau_y \neq \tau_w$, thus, it appears that the assumption that $\tau_y = \tau_w$ when flow ceases is wrong. There are three possible reasons why this might be the case:

1. For these tests τ_y was measured in a rotational viscometer. The rotational viscometer measures fluid shear stress and shear rate in an annulus formed be a stationary cylindrical wall and an inner rotating bob. This subjects the fluid to centrifugal forces that are not present when fluids flow through tubes. Therefore, it may be that the τ_y given by a rotational viscometer is not the correct parameter to use in Eq. (30). Instead τ_y determined in a rotational viscometer may be just an index rather than a physically significant value. A capillary viscometer measures flow properties by flow through a tube of a given diameter, at a known pressure gradient and flow rate. Thus, a capillary viscometer should be used to test the grouts used in the penetration experiments to see if it gives values of τ_y equal to τ_w as determined in Eq. (31).

2. An assumption made in Section I-F was that the grout and in situ fluid are immiscible and that the grout completely displaces the in situ fluid when injected into a tube. Perhaps this assumption is erroneous. In the penetration tests conducted for this study, it may be that air is intermittently trapped along the tube walls and forms a very thin zone that prevents contact of the grout with the tube wall. The air is a Newtonian fluid that has no yield strength and continues

shearing as long as there is any non-zero pressure gradient. Thus, there is a zone of slippage between the wall and the unsheared grout cylinder. When the actual area of grout-wall contact is great enough, the necessary shear force required to counteract the injection pressure force develops and flow ceases. Consequently, the grout will penetrate further in the tube than expected because of slippage in the zone of air along the tube wall. This would explain the results given in Table 3 where the predicted penetration distance is always less than the actual distance for circular tubes, except for test 2. An interesting consequence of this phenomena is suggested. It is often desirable to maximize the size of the grouted mass as much as possible, i.e., to increase the penetration distance for a given grout type and injection pressure.. This could be done by first injecting a Newtonian fluid that has a special affinity for coating the pore walls and is not readily displaced along the walls by injected grout. The Newtonian fluid would then cause slippage of the grout along the pore wall and yield greater penetration distances as happened in these tests.

3. A third possibility is that τ_y may not only be a function of fluid type and preparation but may also be a function of tube size and shape. When L_{max} is plotted versus P_i for a given tube size and shape and τ_y is ignored as done in Figs. 25-28, very good correlation between the variables is obtained as compared to no correlation in Fig. 21 where τ_y is included. If τ_y and τ_w can be explicitly ignored, then it seems that these variables might be dependent on tube size and shape as well as on fluid composition. At the present time this is

only speculation but capillary viscometer tests might demonstrate whether the yield strength of a non-Newtonian fluid is dependent on tube size and shape.

Figures 25-28 also indicate that since data for different tube shapes but similar sizes falls on different lines then a pore shape factor does indeed exist. C can be determined by comparing the L_{max} in a tube of non-circular shape of a given size and at a given injection pressure to L_{max} in a circular tube for the same size and pressure. For example, for a tube hydraulic radius of approximately 0.240 cm (see Fig. 25, R_H = 0.240 cm) we get C = 0.51 for triangular shapes (see Fig. 26, R_H = 0.223 cm) and C = 0.65 for star shape (see Fig. 28, R_H = 0.261 cm). Thus, in order to determine C for other tubes it is necessary to test circular and non-circular tubes of the same R_H at the same injection pressures with the same fluid compositions.

In conclusion, analysis of the data provided by the penetration tests indicates that the concepts involved in the development of the hypothesized equation for predicting penetration distance are correct. However, the value to use for τ_y is not clear. The value of τ_y as determined in the rotational viscometer does not provide the correct results as shown in Table 3. The reason for this is not known at present. It may be due to: (a) shortcomings in the rotational viscometer test; (b) incomplete displacement of air by grout which yields slippage along the tube wall; or (c) a dependence of τ_y on tube shape and size as well as on fluid composition. Tests on the

grouts using a capillary viscometer should be carried out to determine if better results can be obtained. In any case, the main concept involved in the analysis that the non-Newtonian fluid develops a shear force at the tube walls that balances the injection pressure force and prevents flow for a non-zero pressure gradient is confirmed.

Table 3. Results of vertical penetration tests.

Test No.	Tube Shape	Hydraulic Radius R_H (cm)	Pressure Difference $(P_i - P_o)$ (dyne/cm^2)	Yield Strength of Grout τ_y (dyne/cm^2)	Calculated Shear Stress Developed at Tube Wall τ_w (dyne/cm^2)	Actual Length of Penetration L_{max} (cm)	Predicted Length of Penetration $L_{max\ p}$ (cm)
2	circle	0.476	40700	280	277	24.8	24.7
3A	circle	0.476	89600	263	127	68.2	55.6
3B	circle	0.476	131600	263	38.3	115.3	81.6
4A	circle	0.476	108700	147	93.0	93.0	79.4
4B	circle	0.476	140300	188	22.2	126.7	96.4
5A	circle	0.240	109000	227	11.7	111.5	61.7
6A	circle	0.400	109000	280	28.5	96.5	61.9
6B	circle	0.400	168300	280	25.7	150.0	95.6
10B	circle	0.400	146300	410 to 520	26.0	129.7	70.2 or 62.0
10D	circle	0.240	127400	410 to 520	31.5	106.7	46.0 or 39.5
15A	circle	0.400	77800	462	11.0	71.5	35.1
15B	circle	0.400	145300	462	5.5	135.2	65.6
15C	circle	0.400	196400	462	8.4	181.5	88.7
18A	circle	0.240	107600	565	40.6	87.5	31.5
18B	circle	0.240	174000	565	37.3	143.0	51.0
13A	triangle	0.223	36800	502	—	14.8	—
13B	triangle	0.223	90200	502	—	36.9	—
13C	triangle	0.223	157700	502	—	65.7	—
13D	triangle	0.223	222700	502	—	94.2	—
14A	triangle	0.326	31100	464	—	17.4	—
14B	triangle	0.326	103000	464	—	46.0	—
14C	triangle	0.326	165100	464	—	76.6	—
14D	triangle	0.326	230700	464	—	105.0	—

Table 3. Continued.

Test No.	Tube Shape	Hydraulic Radius R_H (cm)	Pressure Difference $(P_i - P_o)$ (dyne/cm^2)	Yield Strength of Grout τ_y (dyne/cm^2)	Calculated Shear Stress Developed at Tube Wall τ_w (dyne/cm^2)	Actual Length of Penetration L_{max} (cm)	Predicted Length of Penetration $L_{max\ p}$ (cm)
16A	rectangle	0.318	59700	465	—	32.3	—
16B	rectangle	0.318	122100	465	—	66.4	—
16C	rectangle	0.318	188300	465	—	103.6	—
16D	rectangle	0.318	257600	465	—	142.6	—
17A	rectangle	0.346	75000	493	—	38.6	—
17B	rectangle	0.346	145600	493	—	79.6	—
17C	rectangle	0.346	214100	493	—	113.5	—
19A	star	0.130	49300	483	—	16.5	—
19B	star	0.130	119800	483	—	40.0	—
19C	star	0.130	192800	483	—	65.4	—
19D	star	0.130	265000	483	—	91.9	—
20A	star	0.174	68900	536	—	31.8	—
20B	star	0.174	134500	536	—	65.5	—
20C	star	0.174	180900	536	—	88.0	—
21A	star	0.261	45100	536	—	24.4	—
21B	star	0.261	96100	536	—	51.0	—
21C	star	0.261	166300	536	—	91.5	—

Note: The specific weight of the grouts used in these tests was 1060 dyne/cm^3.

61

IV. CONCLUSIONS

The purpose of this report has been to develop a method for predicting the maximum penetration distance of a particulate grout with non-Newtonian fluid properties in a porous medium. Once the penetration distance can be predicted, it is then possible to predict the size of a grouted mass in the ground and determine the minimum required grout hole spacing for feasibility studies. A theoretical study has led to the proposal of an equation which can be used to find the penetration distance given the yield strength of the grout, the pressure conditions, and porous medium geometry and characteristics. A brief experimental analysis has been carried out which confirms that the concepts embodied in the equation are valid but that difficulties in determining some of the required parameters have become apparent. The immediate application of this work is for providing a framework for evaluating the feasibility of using a grout composed of spent oil shale for reducing the hydraulic conductivity of in situ oil shale retorts and preventing pollution of surrounding ground water resources. However, the methods proposed here can be used in any engineering application involving grouting of granular material with particulate grouts. Before stating the conclusions of this study, it is useful to restate the assumptions used in the analysis.

A. Assumptions

1. The flow is one-dimensional and horizontal.

2. The fluids and the solid matrix of the porous medium are incompressible.

3. Isothermal conditions are maintained and fluid property changes with change in pressure are insignificant.

4. Cement and clay grouts are non-Newtonian fluids that possess a yield strength. Although some grouts exhibit thixotropy this can be ignored because if grout is kept agitated and is not allowed to "rest" then the grout behaves as a time-independent material.

5. Flowing non-Newtonian fluids with a yield strength possess an unsheared cylinder of material in the center of flow. The size of this unsheared cylinder varies with yield strength and inversely with pressure gradient. For this reason, a non-zero pressure gradient exists, below which flow can not occur in a tube of a given size.

6. The pressure gradient in a tube of constant hydraulic radius is linear.

7. Fluid flow is not limited by fluid supply or available injection time.

8. Water or air and particulate grouts are immiscible fluids with sharp, abrupt interfaces between them in two-phase flow. Grout completely displaces water or air in flow paths as grout in injected.

9. Flow is laminar.

10. Pores in a porous medium can be modelled as many interconnecting, sinuous tubes of varying hydraulic radii and shapes.

11. Surface tension and capillary pressures are insignificant.

B. Conclusions

1. Based on fundamental considerations of non-Newtonian fluid flow, the maximum penetration distance of a particulate grout in a straight, horizontal, circular tube of constant radius is

$$L_{max} = \frac{R(P_i - P_o)}{2 \tau_y}$$

2. Prediction of the penetration distances of Newtonian grouts is given by the Buckley-Leverett equation. However, predictions based on equations developed by Raffle and Greenwood for spherical grouted masses are only applicable to the case where the Newtonian grout (chemical) has nearly the same viscosity and density as the displaced water. Otherwise, these equations are in error because their derivation ignores the phenomena of multi-phase flow and varying hydraulic conductivity with varying saturation. An equation similar to Raffle and Greenwood but for injection of a Newtonian grout from a cylindrical pipe and forming a cylindrical grouted mass has been derived in this report and is

$$t = \frac{n}{(H_1 - H_2) K} \left\{ r^2 \left[\frac{\ln(r/r_0)}{2} - \frac{1}{4} \right] + \frac{r_0^2}{4} \right\}$$

where the grout has nearly the same viscosity and density as water.

3. The Raffle and Greenwood method for predicting penetration distance of a particulate grout is not valid because they used equations which only apply to Newtonian flow to draw conclusions about non-Newtonian flow. When their approach is used based on non-Newtonian fluid flow equations, it fails to provide useful results.

4. Based on a Kozeny-Carman type analysis, Darcy's Law does not apply to particulate grout flow in a porous medium because the hydraulic conductivity of the medium with respect to the grout is not a constant but depends on the pressure gradient. A corollary of this is that with regard to grout flow, porous media do not have an intrinsic permeability that depends only on media properties.

5. The main hypothesis of this report is that the penetration distance of a grout in a sinuous, non-circular, horizontal soil pore is given by

$$L_{max} = \frac{C \, R_H (P_i - P_o)}{T \, \tau_y}$$

where C = pore shape factor that is experimentally determined and depends on the cross-sectional shape of the pore passage and T = tortuosity factor that is a function of the longitudinal geometry of the pore passages. For flow paths of varying hydraulic radii the above equation must be solved using an iterative algorithim that is based on dividing the flow path up into segments of constant hydraulic radius.

6. "Groutability" depends on the yield strength of the grout and pore passage geometry and is not generally a function of particle blockage or ratios between pore dimensions and grout particle size.

7. The hydraulic conductivity of a grouted mass with respect to water varies directly with distance from the injection point. This is because larger voids are left unfilled further from the injection point due to lower critical pressure gradients.

8. In order to use the hypothesized equation proposed in this report, it is necessary that the pore passage geometry be known. Measurement of flow path geometry is not routinely done and presents problems for applying the equation.

9. Injection experiments using a bentonite slurry of Bingham fluid characteristics were carried out at LBL. The purpose of these experiments was to verify the validity of the proposed equation and to determine the pore shape factor for various tube shapes. The tests indicated that the concepts embodied in the hypothesis are valid and the relationships suggested by the proposed equations describe the observed phenomena. However, the experiments revealed that the yield strength of the grout as measured with a rotational viscometer is not the shear stress actually developed at the tube wall when grout flow ceases. This may be due to (a) shortcomings in the rotational viscometer test; (b) incomplete displacement of air by grout which yields slippage along the tube wall; or (c) a dependence of τ_y on tube shape and size as well as on fluid composition. Tests on the grouts using a capillary viscometer should be carried out to determine if better results can be obtained.

BIBLIOGRAPHY

Attewell, P. B. and I. W. Farmer (1976). Principles of Engineering
Geology.

Buckley, S. E. and M. C. Leverett (1942), "Mechanism of Fluid
Displacement in Sands," Transactions of the AIME, Vol. 146,
pp. 107-116.

Beirute, R. M. and R. M. Flumerfelt, "An Evaluation of the Robertson-
Stiff Model Describing Rheological Properties of Drilling Fluids
and Cement Slurries," Society of Petroleum Engineers Journal, vol.
18, April 1977, pp. 79-100.

Duncan, J. M., et al. (1972), "Seepage and Groundwater Effects
Associated with Explosive Cratering," Report TE-72-2 to U. S. Army
Engineer Waterways Experiment Station-Explosive Excavation Research
Office, Chapter 2.

Freeze, R. allan, and John A. Cherry (1979), Groundwater, Chapter 2.

Herndon, Joe and Tom Lenahan (1976). Grouting in Soils: Vol. 1A,
State-of-the-Art Report, Report No. FHWA-RD-76-26 prepared for
Federal Highway Administration, Office of Research and Development.

Hughes, William F. (1979), An Introduction to Viscous Flow, Chapters 1
and 2.

Marsland, A. and A. G. London (1963). The Flow Properties and Yield
Gradients of Bentonite Grouts in Sands and Capillaries" in Grouts
and Drilling Muds in Engineering Practice, pp. 15-21.

Mitchell, J. K. (1970), "In-Place Treatment of Foundation Soils," Journal of the Soil Mechanics and Foundation Division of the ASCE, Vol. 96, No. SM1, January, 1970, pp. 73-110.

Mitchell, J. K. (1976). Fundamentals of Soil Behavior, Chapters 12 and 15.

Morel-Seytoux, H. J. (1969). "Introduction to Flow of Immiscible Liquids in Porous Media," in Flow Through Porous Media, edited by Roger J. M. DeWiest, pp. 456-512.

Raffle, J. F. and D. A. Greenwood (1961), "The Relation Between the Rheological Characteristics of Grouts and Their Capacity to Permeate Soils," Proceedings of the 5th International Conference on Soil Mechanics and Foundation Engineering, pp. 789-793.

Robertson, R. E. and H. A. Stiff, Jr., "An Improved Mathematical Model for Relating Shear Stress to Shear Rate in Drilling Fluids and Cement Slurries," Society of Petroleum Engineers Journal, vol. 17, February 1976, pp. 31-36.

Scheidegger, Adrian E. (1974), The Physics of Flow Through Porous Media.

Skelland, A. H. P. (1976), Non-Newtonian Flow and Heat Transfer.

Thomas, D. G. (1961), "Laminar Flow Properties of Flocculated Suspensions," Journal of the American Institute of Chemical Engineering, Vol. 7, pp. 431-437.

Thomas, D. G. (1963), "Relation of Hindered-Settling Flow Characteristics to Rheological Parameters," Journal of the American Institute of Chemical Engineering, vol. 9, pp. 310-316.

Welge, H. J. (1952), "A Simplified Method for Computing Oil Recovery by Gas or Water Drive," Transactions of the AIME, Vol. 195, pp. 91-98.

Wilkinson, W. L. (1960), Non-Newtonian Fluids--Fluid Mechanics, Mixing and Heat Transfer.

APPENDIX I: DERIVATION OF KOZENY-CARMAN TYPE EQUATIONS FOR
              HYDRAULIC CONDUCTIVITY FOR BINGHAM, CASSON, AND
              HERSCHEL-BULKLEY FLUIDS

The theoretically derived equation for the hydraulic conductivity
of Newtonian fluid flow in a porous medium is known as the Kozeny-Carman
equation (Mitchell, 1976) and is given as

$$K_N = \frac{\gamma_N e^3 S^3}{\mu_N C_o T S_o^2 (1 + e)}$$

where e = void ratio (L^3/L^3),

   S_o = specific wetted surface area per unit volume ($1/L$),

   C_o = pore shape factor (dimensionless),

   T = tortuosity factor (dimensionless),

   γ_N = specific weight of Newtonian fluid (F/L^3),

   μ_N = absolute viscosity of Newtonian fluid ($F\,T/L^2$),

   S = saturation (L^3/L^3),

   K_N = hydraulic conductivity for Newtonian fluid (L/T).

Therefore, we can state that

$$K_N = f(e, S_o, C_o, T, S, \gamma_N, \mu_N)$$

where e, S_o, C_o, T are porous medium properties and S, γ_N, μ_N are
Newtonian fluid properties. Using the same theoretical approach based
on a capillary analogy I will now derive Kozeny-Carman type formulas
for Bingham, Casson, and Herschel-Bulkley non-Newtonian fluids.

For other shapes of cross-section the same form of equation will hold except that we must introduce a shape coefficient, C_s. Therefore,

$$q = C_s a \; \frac{R_H^2 i \gamma_B}{\mu_B} \left[1 - \frac{4\tau_y}{3R_H i \gamma_B} + \frac{1}{3} \left(\frac{\tau_y}{R_H i \gamma_B} \right)^4 \right] \quad .$$

For a bundle of parallel tubes of constant total cross section area A (solids plus voids) but with irregular (i.e., non-circular) pore shapes the area of flow passages filled with fluid is

$$A_f = S \left(\frac{e}{1 + e} \right) A$$

where S = percent saturation (L^3/L^3),

   e = void ratio (L^3/L^3),

   $e/1+e$ = porosity (L^3/L^3),

   A = total area of cross section, voids plus solids (L^2).

It should be realized that this bundle of parallel tubes is considered to be hydraulically equivalent to the porous medium, that is, the flow rate through the bundle of tubes is equal to the flow rate through the porous medium. Now the hydraulic radius of a cross section of area A is $R_H = A_f/P$ where P is the wetted perimeter and A_f is the cross-sectional area of filled flow passages. Therefore, $R_H = A_f L/PL$ where L is the length of the bundle of tubes. In this case $A_f L = V_f$ and $PL = S_o V_s$ giving $R_H = V_f/S_o V_s$ where V_f is the volume of fluid, V_s is the volume of solids, and S_o is the specific wetted surface area per unit volume in the bundle of tubes. For void ratio e we have

$V_f = eV_sS$, which means $R_H = eV_sS/S_oV_s = eS/S_o$. Therefore, the total flow rate through the bundle is

$$Q = \frac{AS\left(\frac{e}{1+e}\right) C_s\left(\frac{eS}{S_o}\right)^2 i\gamma_B}{\mu_B} \left\{1 - \frac{4}{3}\left[\frac{\tau_y}{\left(\frac{eS}{S_o}\right) i\gamma_B}\right] + \frac{1}{3}\left[\frac{\tau_y}{\left(\frac{eS}{S_o}\right) i\gamma_B}\right]^4\right\}$$

or

$$Q = iA\left\{\frac{C_s e^3 S^3 \gamma_B}{\mu_B(1+e) S_o^2}\left[1 - \frac{4}{3}\left(\frac{\tau_y S_o}{eSi\gamma_B}\right) + \frac{1}{3}\left(\frac{\tau_y S_o}{eSi\gamma_B}\right)^4\right]\right\}$$

By analogy with Darcy's Law we get a hydraulic conductivity for a Bingham fluid of

$$K_B = \frac{C_s e^3 S^3 \gamma_B}{\mu_B(1+e) S_o^2}\left[1 - \frac{4}{3}\left(\frac{\tau_y S_o}{eSi\gamma_B}\right) + \frac{1}{3}\left(\frac{\tau_y S_o}{eSi\gamma_B}\right)^4\right]$$

If we replace C_s with $1/C_oT$, where C_o is the pore shape factor and T is the tortuosity factor, we obtain

$$K_B = \frac{e^3 S^3 \gamma_B}{C_o T\mu_B(1+e) S_o^2}\left[1 - \frac{4}{3}\left(\frac{\tau_y S_o}{eSi\gamma_B}\right) + \frac{1}{3}\left(\frac{\tau_y S_o}{eSi\gamma_B}\right)^4\right]$$

Therefore, $K_B = f(e, S_o, C_o, T, \gamma_B, \tau_y, S, i)$. As a check it can be seen that $K_B = K_N$ if $\tau_y = 0$, $\gamma_B = \gamma_N$ and $\mu_B = \mu_n$.

Casson Fluid

The procedure for deriving flow equations and Kozeny-Carman type equations for Casson fluids is similar to that used for Bingham fluids in the previous section. In order to develop the theoretical equation for hydraulic conductivity for a Casson fluid we must start with the average velocity of flow of the fluid through a circular tube. The derivation of this average velocity will be carried out here in some detail because to my knowledge no one else has ever carried out the analysis before.

The relationship between fluid shear stress and shear rate for a Casson fluid in a circular tube, i.e., Poisseuille flow, is (see Fig. 1 and Table 1),

$$\sqrt{\tau} = \sqrt{\tau_y} + \sqrt{\mu_c \ (-dV/dr)}$$

when $-dV/dr > 0$ and $0 \leq \tau \leq \tau_y$ when $-dV/dr = 0$,

where τ = shear stress in fluid (F/L^2),

τ_y = yield strength of fluid (F/L^2),

dV/dr = shear rate $(1/T)$,

μ_c = "apparent" viscosity of Casson fluid $((F \ T/L^2)^{1/2})$.

The average velocity can be found using the general equation relating flow rate Q and shear stress at the capillary wall τ_w presented in Skelland (1967) which is

$$\frac{Q}{\pi R^3} = \frac{1}{\tau_w^3} \int_0^{\tau_w} \tau^2 f(\tau) \ d\tau$$

where   R = radius of capillary (L),

   $f(\tau)$ = shear rate which is a function of the shear stress (1/T).
The assumptions on which this equation is based are that the flow is
laminar, fluid behavior is time-independent, i.e., non-thixotropic and
non-rheopectic, and there is no slip between the fluid and the tube
wall.

   For a Casson fluid we have the following flow conditions across
the capillary:

if $0 \leq r \leq r_p$ then $0 \leq \tau \leq \tau_y$ and $f(\tau) = -dV/dr = 0$

if $r_p \leq r \leq R$ then $\tau_y \leq \tau \leq \tau_w$ and $f(\tau) = -dV/dr = \dfrac{\sqrt{\tau} - \sqrt{\tau_y}^2}{\mu_c}$.

Therefore, the general equation can be written as

$$\frac{Q}{\pi R^3} = \frac{1}{\tau_w^3} \int_0^{\tau_y} (\tau)^2 f(\tau)\, d\tau + \int_{\tau_y}^{\tau} \tau^2 f(\tau)\, d\tau$$

$$= \frac{1}{\tau_w^3} \int_{\tau_y}^{\tau_w} \tau^2 \frac{\left(\sqrt{\tau} - \sqrt{\tau_y}\right)^2}{\mu_c}\, d\tau$$

because $f(\tau) = 0$ in the first integral. Thus,

$$\frac{Q}{\pi R^3} = \frac{1}{\tau_w^3 \mu_c} \int_{\tau_y}^{\tau_w} \tau^2 (\tau - 2(\tau\tau_y)^{1/2} + \tau_y) \, d\tau$$

$$= \frac{1}{\tau_w^3 \mu_c} \int_{\tau_y}^{\tau_w} (\tau^3 - 2\tau^{5/2}\tau_y^{1/2} + \tau^2\tau_y) \, d\tau$$

$$= \frac{1}{\tau_w^3 \mu_c} \left[\frac{\tau^4}{4} \bigg|_{\tau_y}^{\tau_w} - \frac{4}{7} \tau^{7/2} \tau_y^{1/2} \bigg|_{\tau_y}^{\tau_w} \frac{\tau^3}{3} \tau_y \bigg|_{\tau_y}^{\tau_w} \right]$$

$$= \frac{1}{\tau^3 \mu_c} \left(\frac{\tau_w^4}{4} - \frac{\tau_y^4}{4} - \frac{4}{7} \tau_w^{7/2} \tau_y^{1/2} + \frac{4}{7} \tau_y^4 + \frac{\tau_w^3 \tau_y}{\tau} - \frac{\tau_y^4}{3} \right)$$

$$\frac{Q}{\pi R^3} = \frac{1}{\mu_c} \left(\frac{\tau_w}{4} - \frac{4}{7} (\tau_w \tau_y)^{1/2} + \frac{\tau_y}{3} \right) + \left(\frac{1}{\tau_w^3} - \frac{1}{84} \tau_y^4 \right)$$

$$= \frac{1}{\mu_c} \left(\frac{\tau_w}{4} - \frac{4}{7} (\tau_w \tau_y)^{1/2} + \frac{\tau_y}{3} - \frac{\tau_y^4}{84} \tau_w^3 \right)$$

Since

$$\tau_w = \frac{R i \gamma}{2}$$

where i = hydraulic gradient (L/L),

γ = specific weight of fluid (F/L^3), and

$V_{avg} = Q/\pi R^2$,

Therefore

$$V_{avg} = \frac{R}{\mu_c} \left(\frac{Ri\gamma}{8} - \frac{4}{7} \left(\frac{Ri\gamma}{2} \tau_y \right)^{1/2} + \frac{\tau_y}{3} - \frac{2}{21} \frac{\tau_y^4}{Ri_\gamma^3} \right)$$

As a check, if $\tau_y = 0$ and $\mu_c = \mu_N$, then V_{avg} for Casson $= R^2 i\gamma/8\mu_c = V_{avg}$ for Newtonian fluid.

Now that we have V_{avg} we can obtain a Kozeny-Carman type equation for the hydraulic conductivity of a porous medium with respect to a Casson fluid. The procedure used in the derivation is exactly the same as that used in the previous section for a Bingham fluid. Consequently, the derivation in this section will be abbreviated and symbols used in the previous section will be used here.

The flow rate of a Casson fluid in a circular tube of cross-sectional area "a," with hydraulic radius $R_H = R/2$, and with pore snape coefficient C_S is

$$q = C_S a V_{avg}$$

$$= C_S a \frac{2R_H}{\mu_c} \left(\frac{R_H i\gamma}{4} - \frac{4}{7} (R_H i\gamma \tau_y)^{1/2} + \frac{\tau_y}{3} - \frac{\tau_y^4}{84(Ri_\gamma)^3} \right)$$

Letting $R_H = eS/S_o$, $C_S = 1/C_o T$, and multiplying numerator and denominator by i we obtain the flow rate through the porous medium of cross sectional area A as

$$Q = iAS \left(\frac{1}{1+e}\right) \frac{2e}{C_0 T \mu_c} \left(\frac{eSi\gamma}{4S_0} - \frac{4}{7} \left(e \frac{Si\gamma}{S_0} \tau_y\right)^{1/2} + \frac{\tau_y}{3} - \frac{\tau_y^4 S_0^3}{84(eSi\gamma)^3} \right)$$

By analogy with Darcy's Law we get a hydraulic conductivity for a Casson fluid of

$$K_c = \frac{e^2 S^2}{C_0 T \mu_c S_0 i (1+e)} \left[\frac{eSi\gamma}{4S_0} - \frac{4}{7} \left(e\frac{Si\gamma\tau_y}{S_0}\right)^{1/2} + \frac{\tau_y}{3} - \frac{\tau_y^4 S_0^3}{84(eSi\gamma)^3} \right]$$

Writing in more abstract terms we have $K_c = f(e, S_0, C_0, T, S, \gamma, \mu_c, \tau_y, i)$.

Herschel-Bulkley Fluid

Again, the procedure used to develop a Kozeny-Carman type equation for Herschel-Bulkley fluids is similar to that used for Bingham fluids in the previous section.

The average velocity for flow of a H-B fluid in a circular capillary is (Skelland, 1967).

$$V_{avg} = \frac{(ri\gamma - 2\tau_y)^{m+1}}{R^2(i\gamma)^3 \mu^m 2^{m-2}} \left[\frac{(Ri\gamma - 2\tau_y)^2}{4(m+3)} + \tau_y \frac{(Ri\gamma - 2\tau_y)}{m+2} + \frac{\tau_y^2}{m+1} \right]$$

when $\tau = \tau_y + \mu(-dV/dr)^{1/m}$,

where τ_y = yield strength (F/L^2),

μ_{H-B} = apparent viscosity of H-B fluid $(F/L^2 \ T^{1/m})$,

dV/dr = shear rate $(1/T)$,

m = characteristic constant with $m \geq 1$ (dimensionless).

Following the procedure used before we can now derive a Kozeny-Carman equation using the same symbols used in the preceding section.

The flow rate of a Herschel-Bulkley fluid in a circular tube with cross-sectional area "a," with hydraulic radius $R_H = R/2$, and with pore shape coefficient C_S is

$$q = C_S a V_{avg}$$

$$= \frac{C_S a 2 (R_H i\gamma - \tau_y)^{m+1}}{R_H^2 (i\gamma)^3} \left[\frac{(R_H i\gamma - \tau_y)^2}{(m+3)} + \frac{2\tau_y (R_H i\gamma \tau_y)}{m+2} + \frac{\tau_y^2}{m+1} \right]$$

Letting $R_H = eS/S_0$, $C_S = 1/C_0 T$, and multiplying numerator and denominator by i we obtain the flow rate through the porous medium of cross sectional area A as

$$Q = iA \frac{S\left(\frac{1}{1+e}\right) 2(eSi\gamma - S_0\tau_y)^{m+1}}{C_0 T(eS)^2 i^4 \gamma^3 \mu_{H-B}^m S_0^{m-1}} \left[\frac{(eSi\gamma - S_0\tau_y)^2}{S_0(m+3)} \right.$$

$$\left. + \frac{2\tau_y(eSi\gamma - S_0\tau_y)}{S_0(m+2)} + \frac{\tau_y}{m+1} \right]$$

By analogy with Darcy's Law we get a hydraulic conductivity for a Herschel-Bulkley fluid of

$$K_{HB} = \frac{S(eSi\gamma - S_o\tau_y)^{m+1}}{C_oT(eS)^2 \; i^4 \gamma^3 \mu^m S_o^{m-1}(1+e)} \left[\frac{(eSi\gamma - S_o\tau_y)^2}{S_o^2(m+3)} \right.$$

$$\left. + \frac{2\tau_y(eSi\gamma - S_o\tau_y)}{S_o(m+2)} + \frac{\tau_y^2}{m+1} \right]$$

Writing in more abstract terms we get

$$K_{H-B} - f(e,S_o,C_o,T,S,\gamma,\mu_{H-B},\tau_y,m,i) \qquad .$$

Summary

For the following fluids we have these Kozeny-Carman type equations to express the hydraulic conductivity of the fluid in a porous medium.

Newtonian Fluid

$$K_N = \frac{\gamma_N e^3 S^3}{\mu_n C_o TS_o(1+e)}$$

$$K_N = f(e,S_o,C_o,T,S,\gamma_N,\mu_N)$$

Bingham Fluid

$$K_B = \frac{e^3 S^3 \gamma_B}{C_o T \mu_B(1+e) \, S_o^2} \left[1 - \frac{4}{3} \; \frac{S_o\tau_y}{eSi\gamma_B} + \frac{1}{3}\left(\frac{S_o\tau_y}{eSi\gamma_B} \right) \right]$$

$$K_B = f(e,S_o,C_o,T,S,\gamma_B,\mu_B,\tau_y,i)$$

Casson Fluid

$$K_C = \frac{e^2 S^2}{C_0 T \mu_c S_0 i (1 + e)} \left[\frac{eSi\gamma_c}{4S_0} - \frac{4}{7} \left(\frac{eSi\gamma_c \tau_y}{S_0} \right)^{1/2} + \frac{\tau_y}{3} - \frac{\tau_y^4 S_0^3}{84(eSi\gamma_c)^3} \right]$$

$$K_C = f(eS_0, C_0, T, S, \gamma_c, \mu_c, \tau_y, i)$$

Herschel–Bulkley Fluid

$$K_{H-B} = \frac{S(eSi\gamma - S_0\tau_y)^{m+1}}{C_0 TeS^2 i^4 \gamma^3 \mu^m S^{m-1}(1 + e)} \left[\frac{(eSi - S_0\tau_y)^2}{S_0^2 (m + 3)} \right.$$

$$\left. + \frac{2\tau_y(eSi\gamma - S_0\tau_y)}{S_0(m + 2)} + \frac{\tau_y}{m + 1} \right]$$

$$K_{H-B} = f(e, S_0, C_0, T, S, \gamma, \mu, \tau_y, m, i) \quad .$$

APPENDIX II. DERIVATION OF EQUATION FOR DETERMINING DISTANCE
OF PENETRATION OF NEWTONIAN GROUT ASSUMING GROUTED
MASS IS A CYLINDER

This theoretical derivation of the penetration distance of a

Newtonian grout is based on a procedure given in Herndon and Lenahan

(1976). They showed the steps and assumptions involved in obtaining

Raffle and Greenwood's (1961) equation

$$t = \frac{nr_0^2}{h_1 K} \left\{ \frac{N}{3} \left[\left(\frac{r}{r_0}\right)^3 - 1 \right] - \frac{N-1}{2} \left[\left(\frac{r}{r_0}\right)^2 - 1 \right] \right\}$$

where t = time of injection (T),

   n = soil porosity (L^3/L^3),

   r_0 = radius of injection pipe (L),

   h_1 = grouting pressure head at the top of the pipe (L),

   K = hydraulic conductivity of soil with respect to water (L/T),

   N = ratio of grout viscosity to water viscosity, i.e.,

   $\gamma_w \mu_g / \gamma_g \mu_w$,

   r = distance of penetration of grout (L).

As mentioned in the main body of the report, this equation is only

applicable for the special case where the Newtonian grout viscosity

and density is nearly the same as water. Also it is assumed that the

grouted mass will be a sphere of radius, r, and that the injection

source is a very small sphere of radius, r_0. In actual fact, the

grout is often injected from a short length of pipe so that the source

is a cylinder rather than a sphere. Also, grouted masses often appear

to be cylindrical in shape with the length of the grouted mass being

approximately the same length as the pipe (Karol, 1968). Therefore, I have chosen to derive a similar expression for cylindrically shaped grouted masses.

Let us assume that the length of the grout injection pipe is L with pipe radius r_o. Let us further assume that the grouted mass has length L and radius r. Then the grouting flow rate at the surface of the grouted cylinder is

$$Q = (2\pi rL)V_r$$

where V_r is the radial flow velocity across a unit area. Using Darcy's Law we see that

$$V_r = - K_g \frac{\partial h}{\partial r}$$

where $\frac{\partial h}{\partial r}$ = hydraulic gradient at r,

K_g = hydraulic conductivity of medium with respect to the Newtonian grout.

If the Newtonian grout has viscosity and density nearly the same as water then K_g = K where K is conductivity with respect to water. Therefore, the velocity of propagation of the grout front is

$$V_r = -K \frac{\partial h}{\partial r}$$

Then

$$Q = (2\pi rL) -K \frac{\partial h}{\partial r}$$

Rearranging gives

$$\partial h = - \frac{Q}{2\pi KL} \frac{\partial r}{r}$$

Integration gives

$$h = - \frac{Q}{2\pi KL} \ln(r) + C$$

where h = hydraulic head at radius r. When $r = r_0$, $h = h_1$ = grout
injection pressure head. Thus

$$C = h_1 + \frac{Q}{2\pi KL} \ln(r_0)$$

then

$$h = - \frac{Q}{2\pi KL} \ln(r) + \frac{Q}{2\pi KL} \ln(r_0) + h_1$$

$$h = \frac{Q}{2\pi KL} \ln \left(\frac{r_0}{r}\right) + h_1$$

Let "r_n = radius of cylinder of influence, beyond which the hydraulic
gradient is unchanged" (Herndon, Lenahan, 1976). We can recalculate

the constant of integration by saying that at $r = r_n$, $h = h_2 =$ in situ hydraulic head. Thus,

$$C = h_2 + \frac{Q}{2\pi KL} \ln(r_n)$$

then

$$h = \frac{Q}{2\pi KL} \ln\left(\frac{r_n}{r}\right) + h_2$$

then

$$\frac{Q}{2\pi KL} \ln\left(\frac{r_o}{r}\right) + h_2 = \frac{Q}{2\pi KL} \ln\left(\frac{r_o}{r}\right) + h_1$$

Now when r is large, say, several times larger than r_o, then $h = h_2$ which means that $r = r_n$. Thus the above equation becomes

$$\frac{Q}{2\pi KL} \ln\left(\frac{r_n}{r_n}\right) + h_2 = \frac{Q}{2\pi KL} \ln\left(\frac{r_o}{r}\right) + h_1$$

and

$$h_1 - h_2 = -\frac{Q}{2\pi KL} \ln\left(\frac{r_o}{r}\right)$$

$$h_1 - h_2 = \frac{Q}{2\pi KL} \ln\left(\frac{r}{r_o}\right)$$

This equation does not show the time required for grout to reach a particular radius. The rate of change of the radius with time $dr/dt = V_r/n$ where n = soil porosity.

$$\frac{dr}{dt} = \frac{Q}{2\pi r L n} = \frac{(h_1 - h_2) KL}{\ln(r/r_0)} \frac{1}{rLn}$$

thus

$$dt = \frac{n}{(h_1 - h_2) K} r \ln\left(\frac{r}{r_0}\right) dr$$

$$t = \int dt = \frac{1}{(h_1 - h_2) K} \int r \ln\left(\frac{r}{r_0}\right) dr$$

$$t = \frac{n}{(h_1 - h_2) K} \left\{ r^2 \frac{\ln(r/r_0)}{2} - 1/4 \right\} + C$$

At $t = 0$, $r = r_0$

$$C = \frac{n}{(h_1 - h_2) K} \left\{ r_0^2 [0 - 1/4] \right\}$$

$$C = \frac{n}{(h_1 - h_2) K} \frac{r_0^2}{4}$$

thus

$$t = \frac{n}{(h_1 - h_2) K} \left\{ r^2 \left[\frac{\ln(r/r_0)}{2} - 1/4 \right] + \frac{r_0^2}{4} \right\}$$

or, expressed in terms of radius,

$$r^2\left[\frac{\ln(r/r_0)}{2} - 1/4\right] = \frac{t(h_1 - h_2) \, K}{n} - \frac{r_0^2}{4}$$

Thus we have a relationship between radius of grout cylinder versus time of injection for given conditions of grout pipe radius, injection head, in situ head, ratio of grout kinematic viscosity to water viscosity, soil hydraulic conductivity with respect to water, and porosity for Newtonian grouts. This relationship can be used to predict radius of grouted cylinders for feasibility studies.

Fig. 1. Flow curves for Newtonian and some typical non-Newtonian fields.
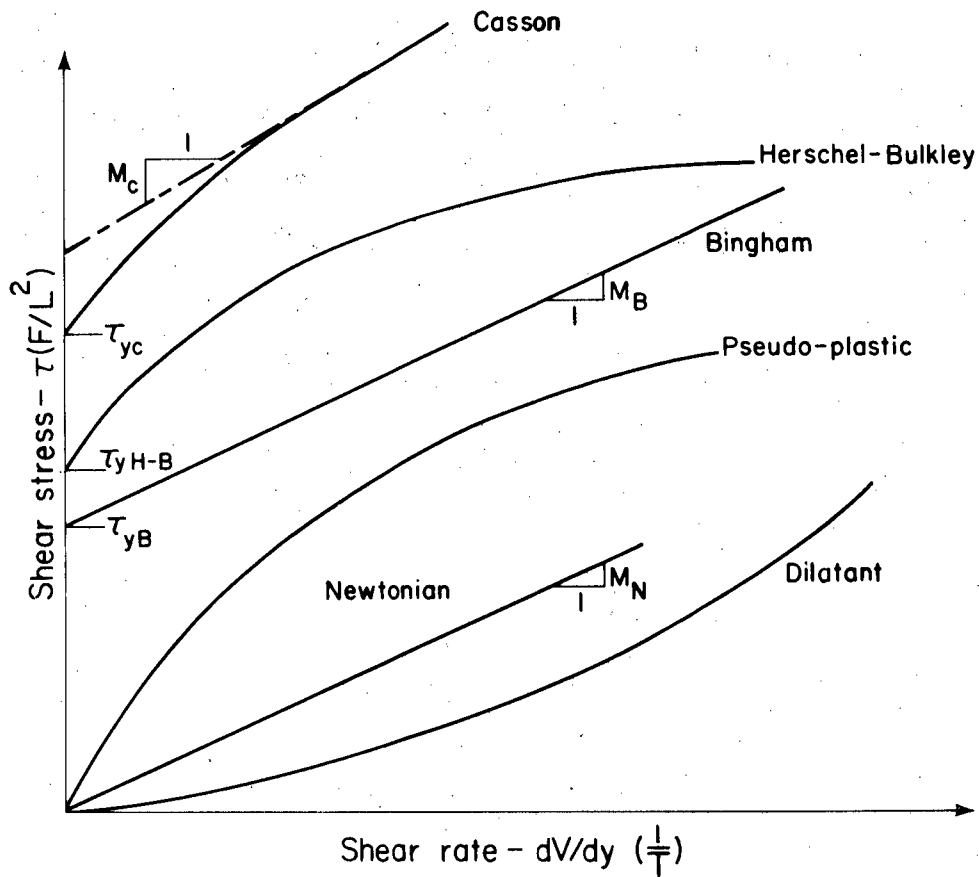
FXBL 8010-2098

Fig. 2. Newtonian fluid flow in a straight, circular, horizontal tube.
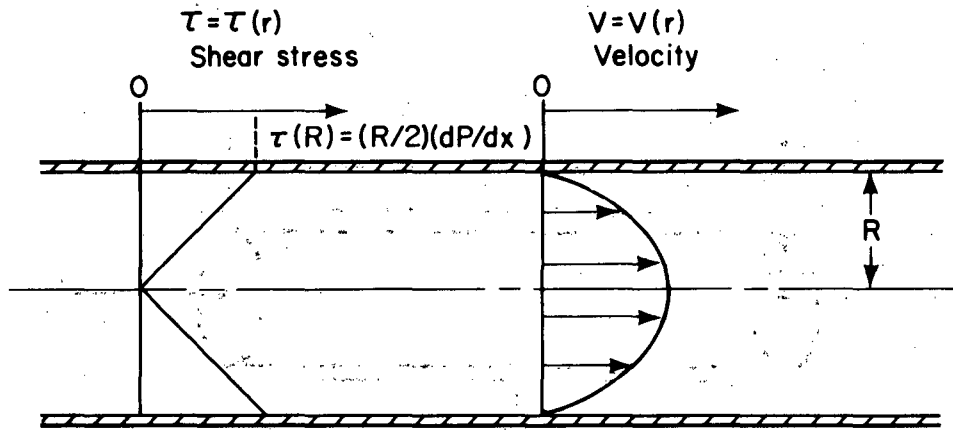
FXBL 8010-2111

For Newtonian fluid flow the flow rate is given by

$$Q = \frac{\pi R^4 \ (dP/dL)}{8\mu}$$

where Q = flow rate; R = tube radius; dP/dL = pressure gradient
and μ = absolute viscosity.

The following assumptions apply:

1. Flow is laminar and steady.
2. Fluid is time-independent.
3. At $r = 0$, $dV/dr = 0$ and $\tau(0) = 0$
4. At $r = R$, $V(R) = 0$ and $\tau(R) = (R/2)/(dP/dL)$.

Fig. 3. An overall force balance on a cylindrical fluid element in a
circular tube flowing at constant velocity.
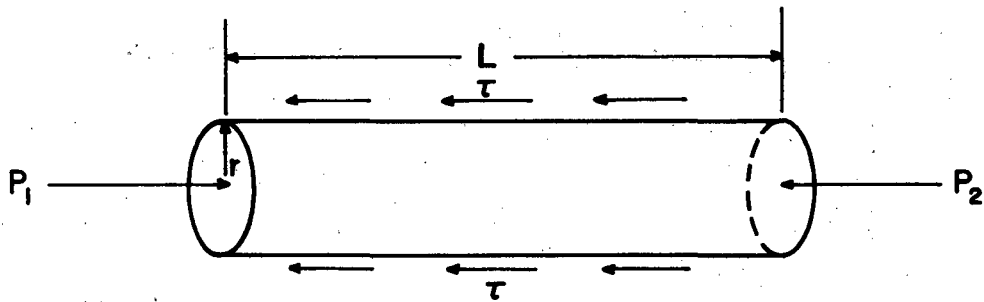
XBL 819-2008

The overall force balance for the fluid cylinder shown
above when at a constant velocity is

$$P_1 \pi r^2 - P_2 \pi r^2 - \tau 2 \pi r L = 0$$

or

$$\tau = \tau(r) = \frac{P_1 - P_2}{L} \cdot \frac{r}{2}$$

If r = R = tube radius, then the shear stress at the tube
wall

$$= \tau_w = \tau(R) = \frac{P_1 - P_2}{L} \cdot \frac{R}{2}$$

Fig. 4. Non-Newtonian fluid flow in a circular tube with an unsheared cylinder occurring at the center of the tube.
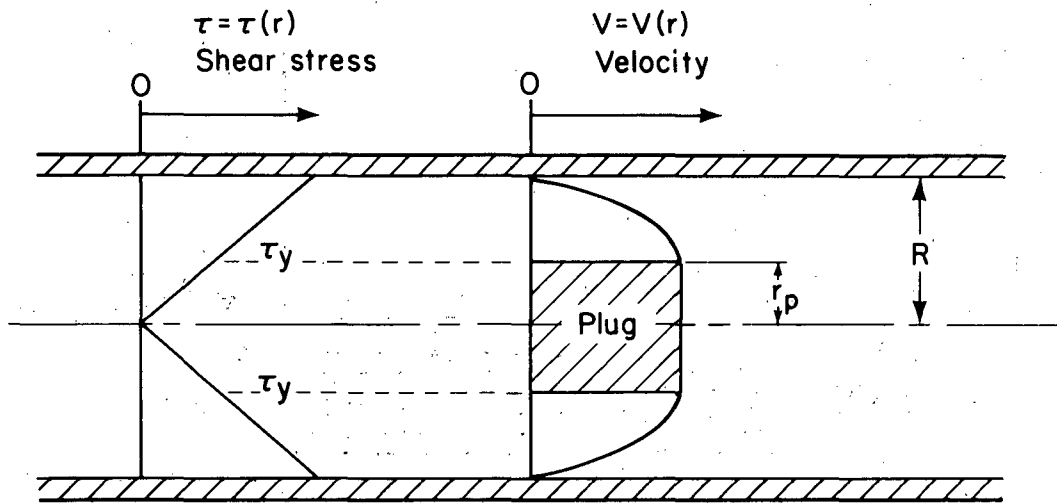
FXBL 8010-2108

For a non-Newtonian fluid with a yield strength - τ_y - flowing in a straight, circular tube with a constant velocity, an unsheared cylinder developed in the center of the tube. This unsheared cylinder forms because the shear stress in the central zone of the tube is less than τ_y, and, therefore, the fluid does not undergo shear deformation. The radius of the unsheared cylinder is

$$r_c = \frac{2\,\tau_y}{(dP/dL)} = \frac{2\,\tau_y}{G}$$

where $G = dP/dL$ = pressure gradient. Obviously, if $r_c = R$, then flow ceases. Conversely, the critical pressure gradient at which flow ceases is given by

$$G_c = \frac{2\,\tau_y}{R}$$

92

Fig. 5. Steady state flow of a non-Newtonian fluid between two
reservoirs.
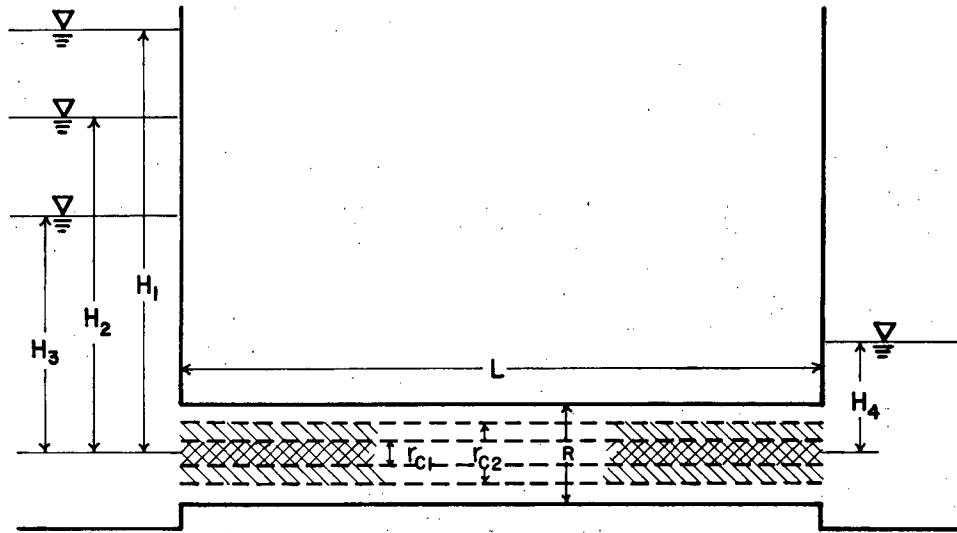
XBL 819-2009

Fig. 6. Injection of a non-Newtonian grout into a water-filled,
straight, circular tube.
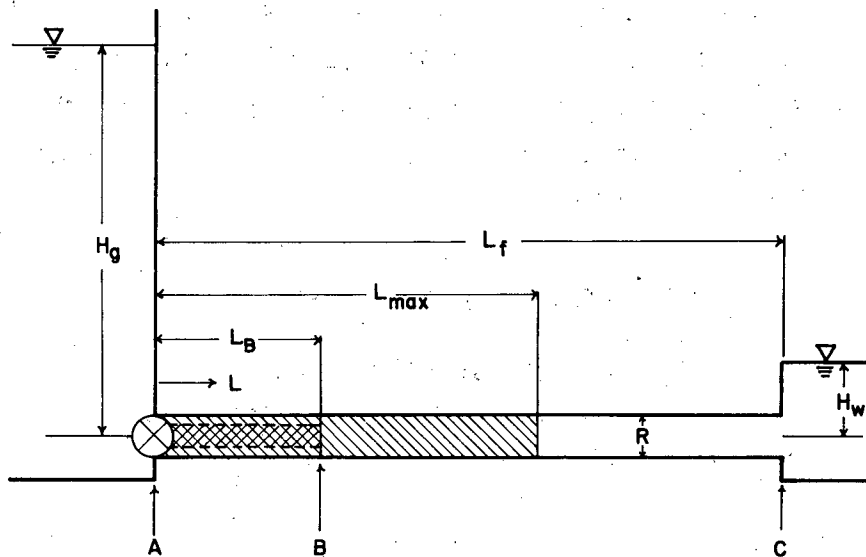
XBL 819-2010

Fig. 7. Relationship between pressure head and distance from the injection point for grout flowing in a straight, circular, horizontal tube.

DISTANCE TO THE GROUT FRONT
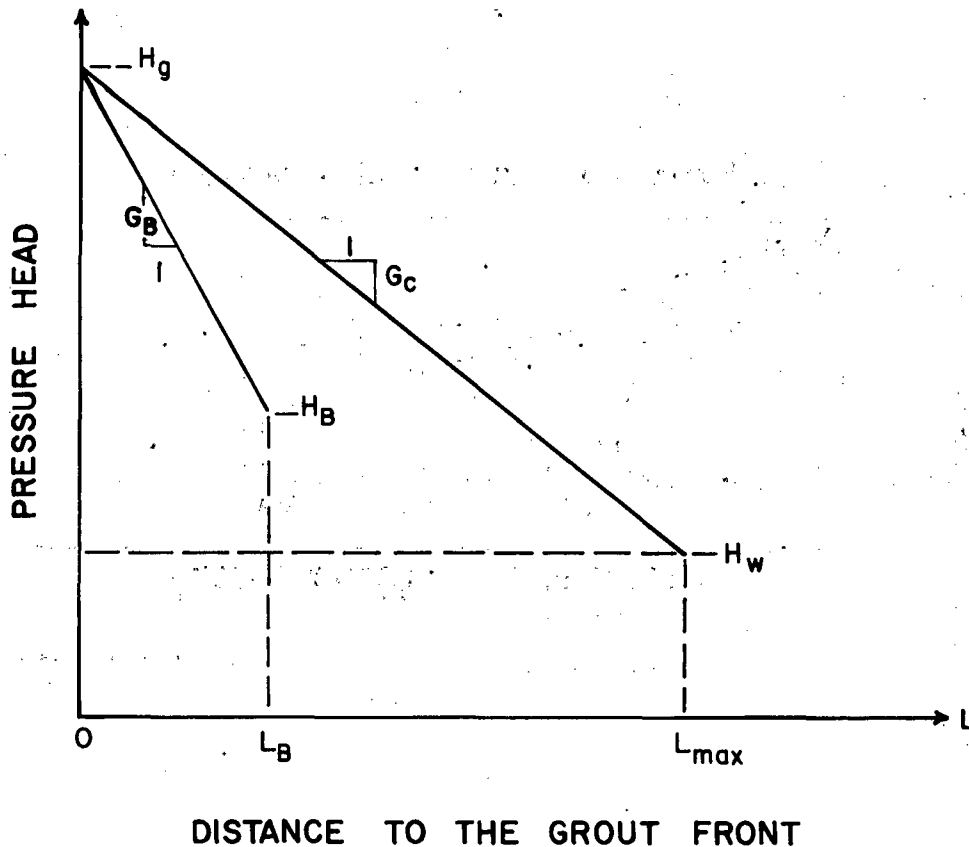
XBL 819-2011

Refer to Figure 6. When the grout front is at point B the pressure gradient in the grout is $G_B = \gamma_g(H_g-H_g)/L_B$. At any point L where $0 < L < L_{max}$ we have $G_L = \gamma_g(H_g-H_L)/L$. As the grout front moves to the right G_L must constantly decrease until flow stops when the critical pressure gradient $G_c = \gamma_g(H_g-H_w)/L_{max} = 2\ \tau_y/R$ is reached.

94

Fig. 8. Example of a Buckley-Leverett saturation profile as it
evolves with time.
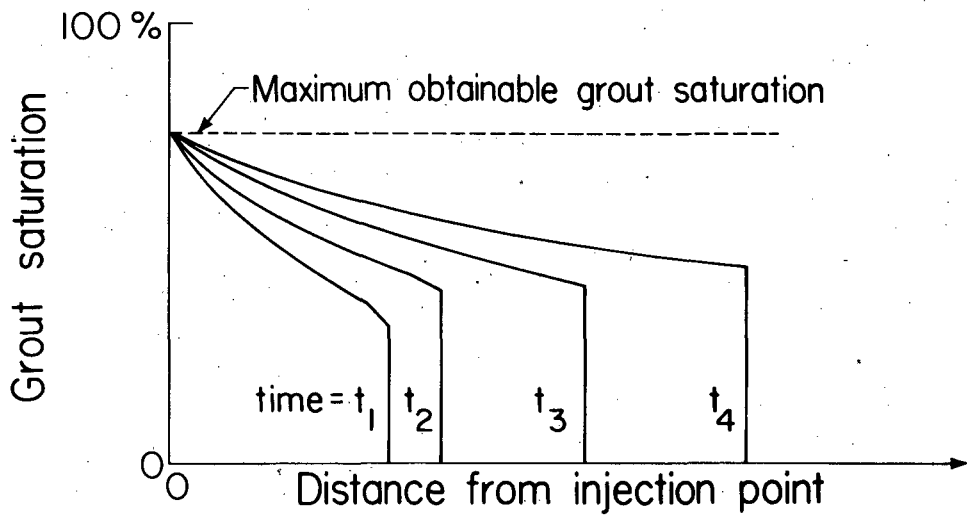
FXBL 8010-2102

Fig. 9. Conceptual model of a bundle of parallel tubes which is
hydraulically equivalent to a porous medium.
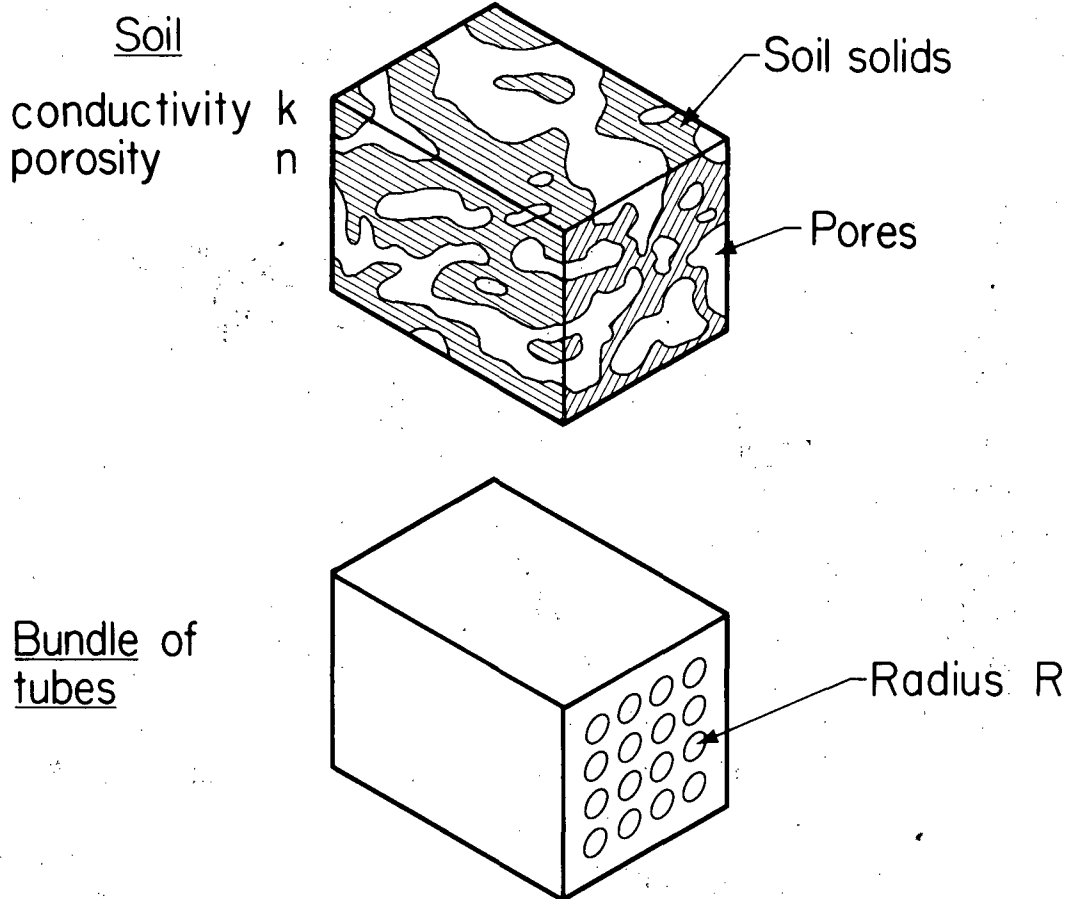
FXBL 8010-2103

The total cross-sectional area of the two models is equal and
the area of flow in the bundle is A·n, therefore, the velocity
of flow in each tube is V/n where V is the Darcy velocity. R,
the tube radius is

$$R = \sqrt{\frac{8 \mu K}{n \gamma}}$$

where γ = fluid specific weight and μ = absolute viscosity of
the fluid.

Fig. 10. Seepage velocity versus hydraulic gradient for bentonite
slurries flowing through uniformly graded sands; generalized
from Marsland and Loudon (1963).
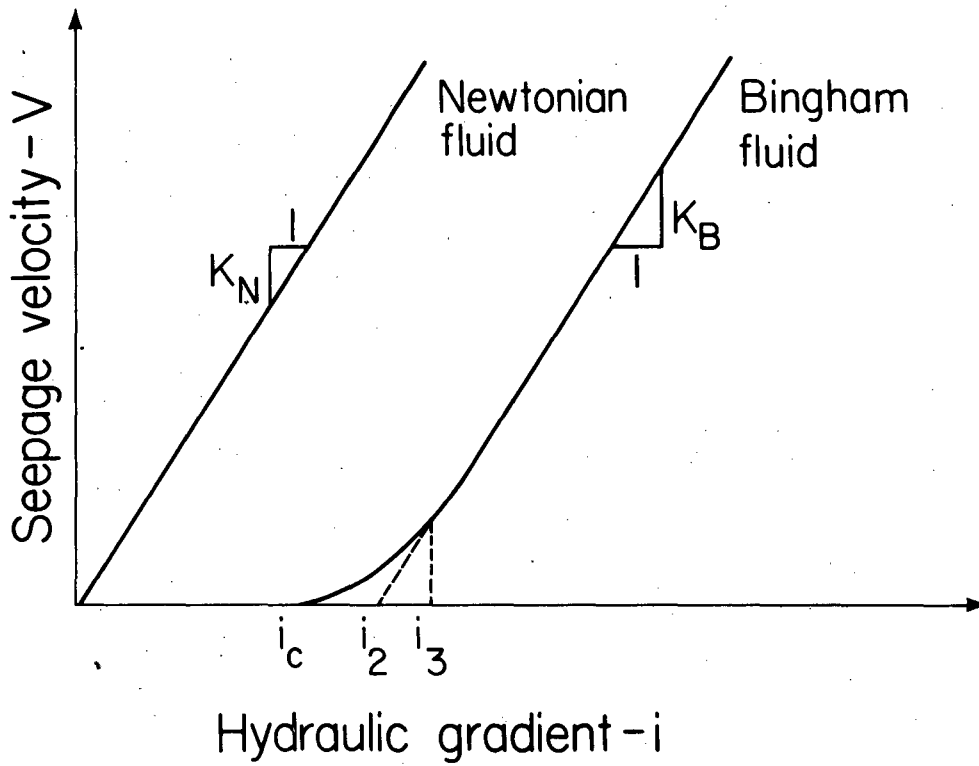
FXBL 8010-2100

Fig. 11. Geometric definition of Tortousity Factor – T.

INJECTION PIPE

L_S

L_{max}
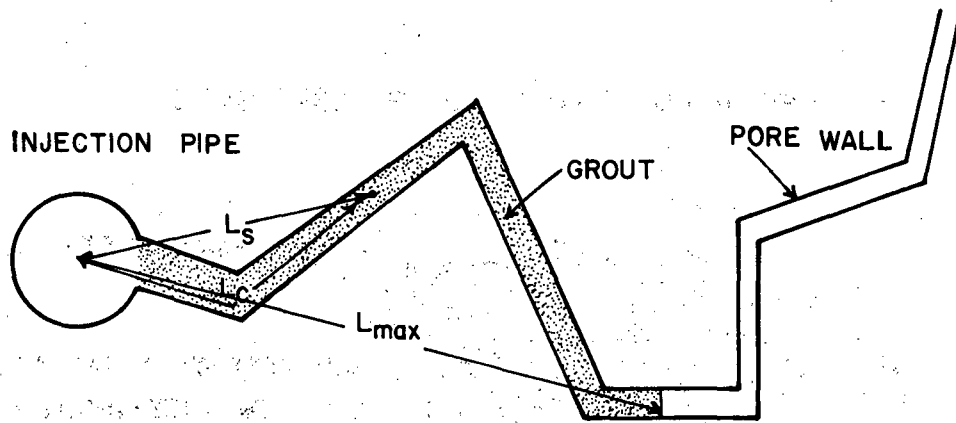
GROUT

PORE WALL

XBL 819-2012

T = Tortuosity Factor = $\dfrac{L_c}{L_s}$ (average) for all points along the pore passage where L_c = actual length of contact between grout and pore wall and L_s = shortest horizontal distance between pipe and point in question (sketch not to scale).

Fig. 12. Definition of Pore Shape Factor for pore passages with
non-circular cross-sections.

SECTION THROUGH A PORE PASSAGE

SOLID PARTICLES

BOUNDARY OF UNSHEARED
CYLINDER AT VARIOUS
PRESSURE GRADIENTS
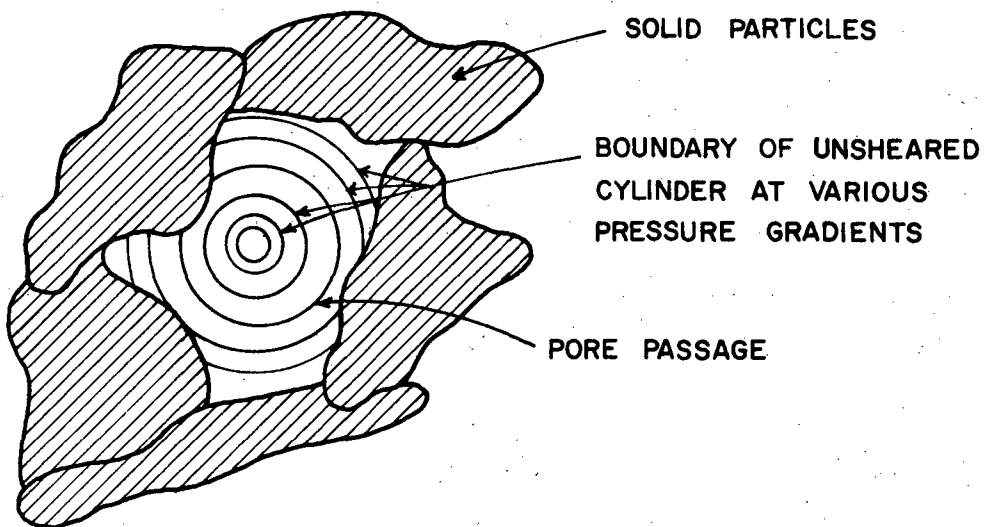
PORE PASSAGE

XBL 819-2013

Pore Shape Factor = C = $\dfrac{L_{max} \text{ in non-circular tube}}{L_{max} \text{ in circular tube}}$

when both tubes have the same R_H and the same fluid is
injected into both tubes at the same pressure.

Fig. 13. Model of a pore passage with varying hydraulic radii and pore shape factor along its length.

XBL 819-1993
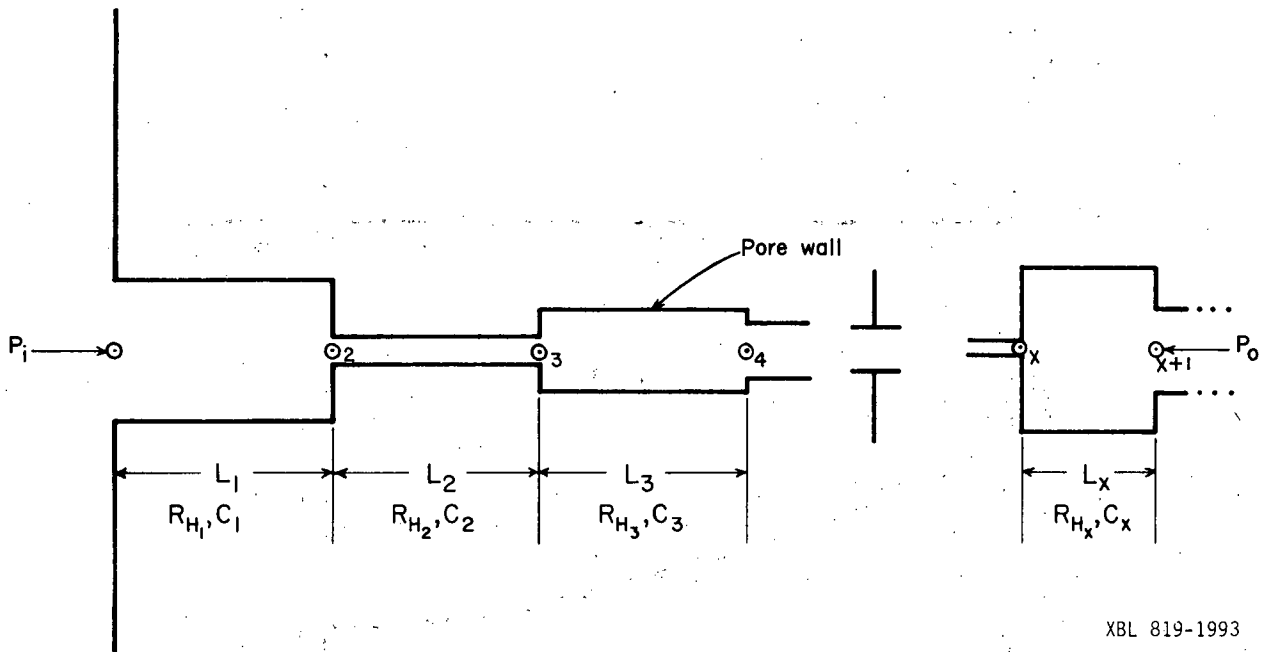
Fig. 14. Conjectural relationships of minimum pore radius, saturation
of pores with grout, and hydraulic conductivity with distance
from injection point.

Distance from injection point
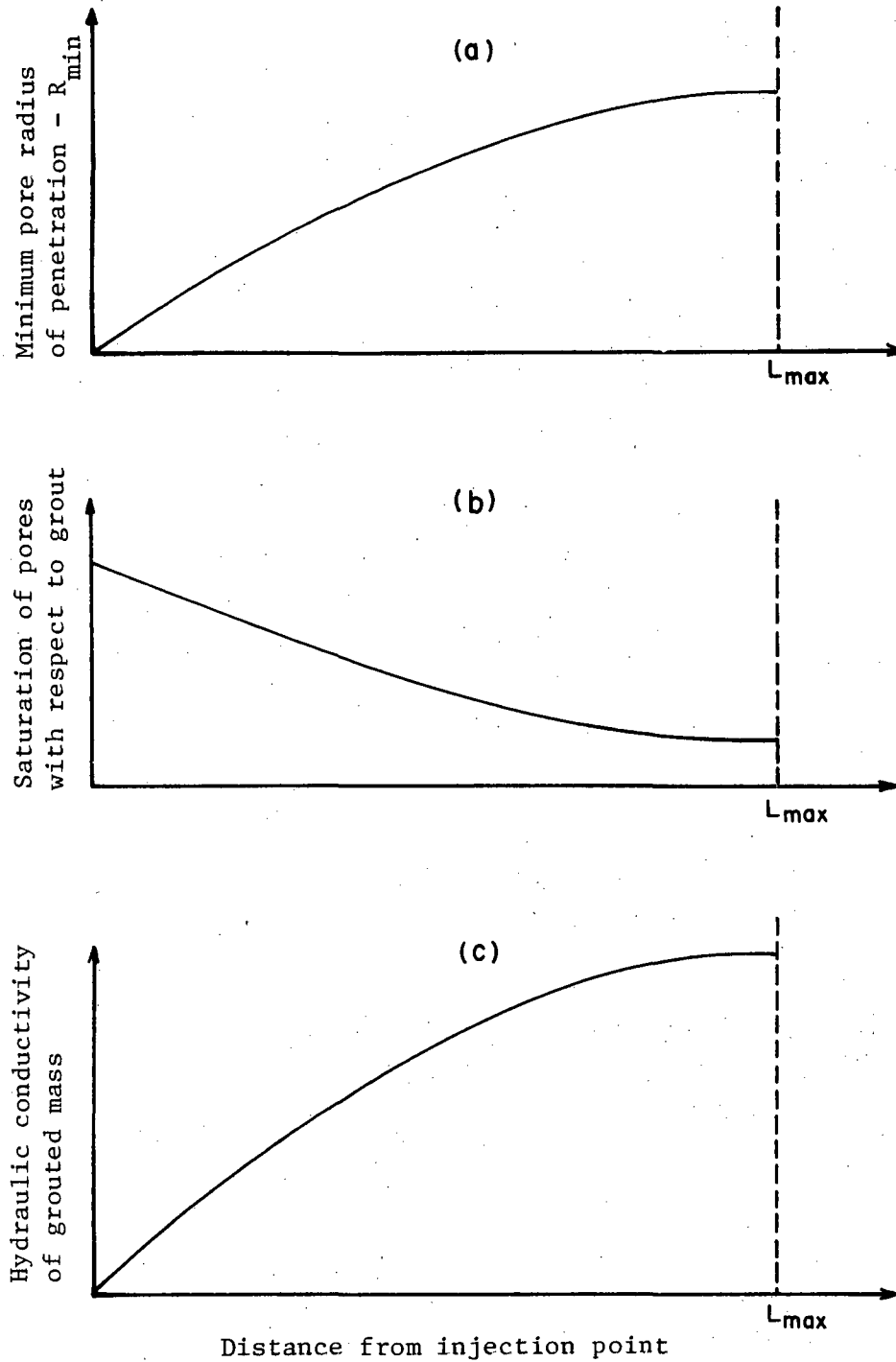
XBL 819-1994

Fig. 15. Sketch of a section through a grouted mass in a porous medium containing a wide range in pore sizes.
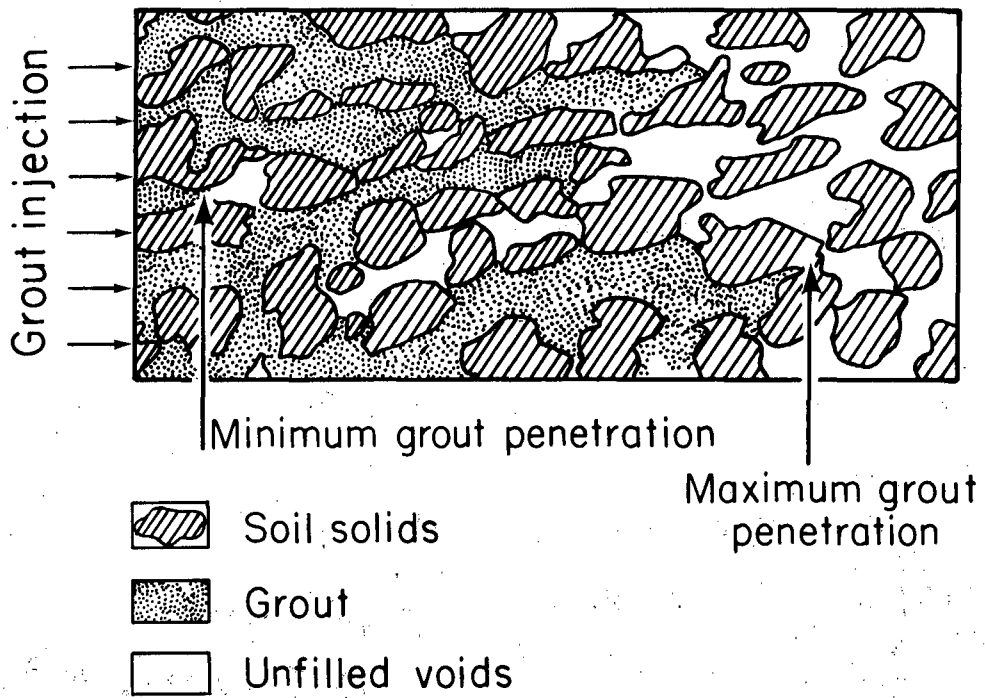
XBL811-47

Fig. 16. Sketch of experimental set-up.
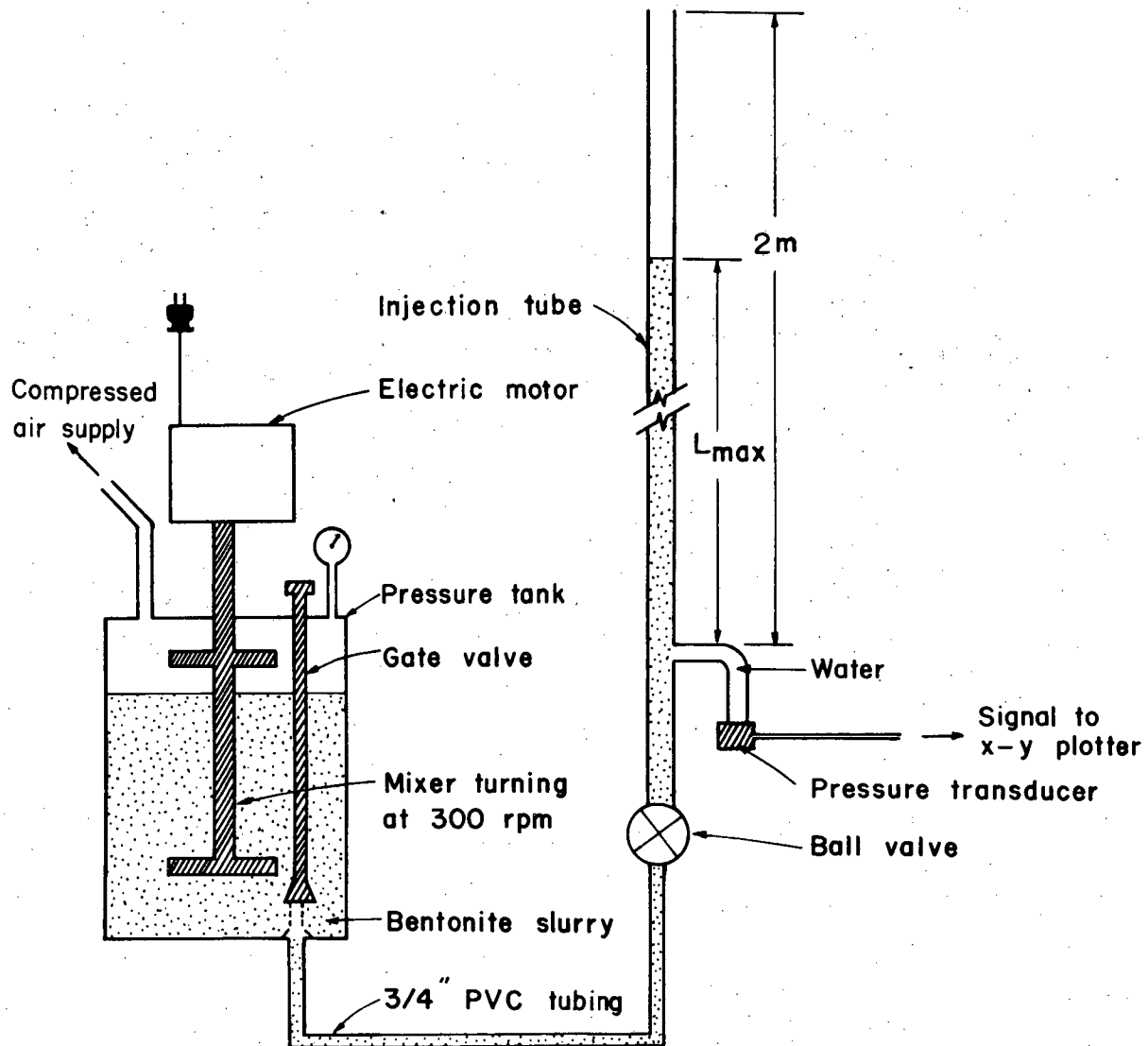
XBL 819-1999

Fig. 17. Cross-sections of tubes used in penetration tests.
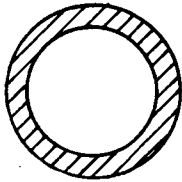
CIRCLE

R_H= 0.240, 0.400, and 0.476 cm
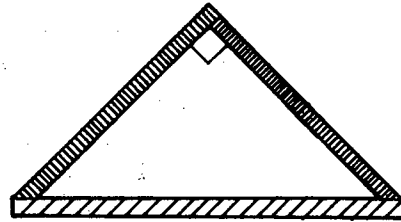
TRIANGLE

R_H= 0.223 , 0.326 cm

RECTANGLE

R = 0.318, 0.346 cm
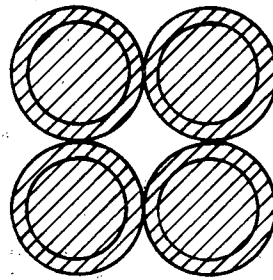
STAR

R = 0.130, 0.174, and 0.261 cm

XBL 819-2000

Fig. 18. Typical circular injection tube design, R_H = 0.240 cm = 0.094 in.

80″

1$\frac{1}{2}$″ Lucite rod

$\frac{1}{4}$″ I.D. Lucite tube

6″

$\frac{3}{8}$″ I.D. Lucite tube

1$\frac{1}{2}$″ Lucite rod

Tap to fit $\frac{3}{4}$″ NPT close nipple

Scale: 1″= 1″
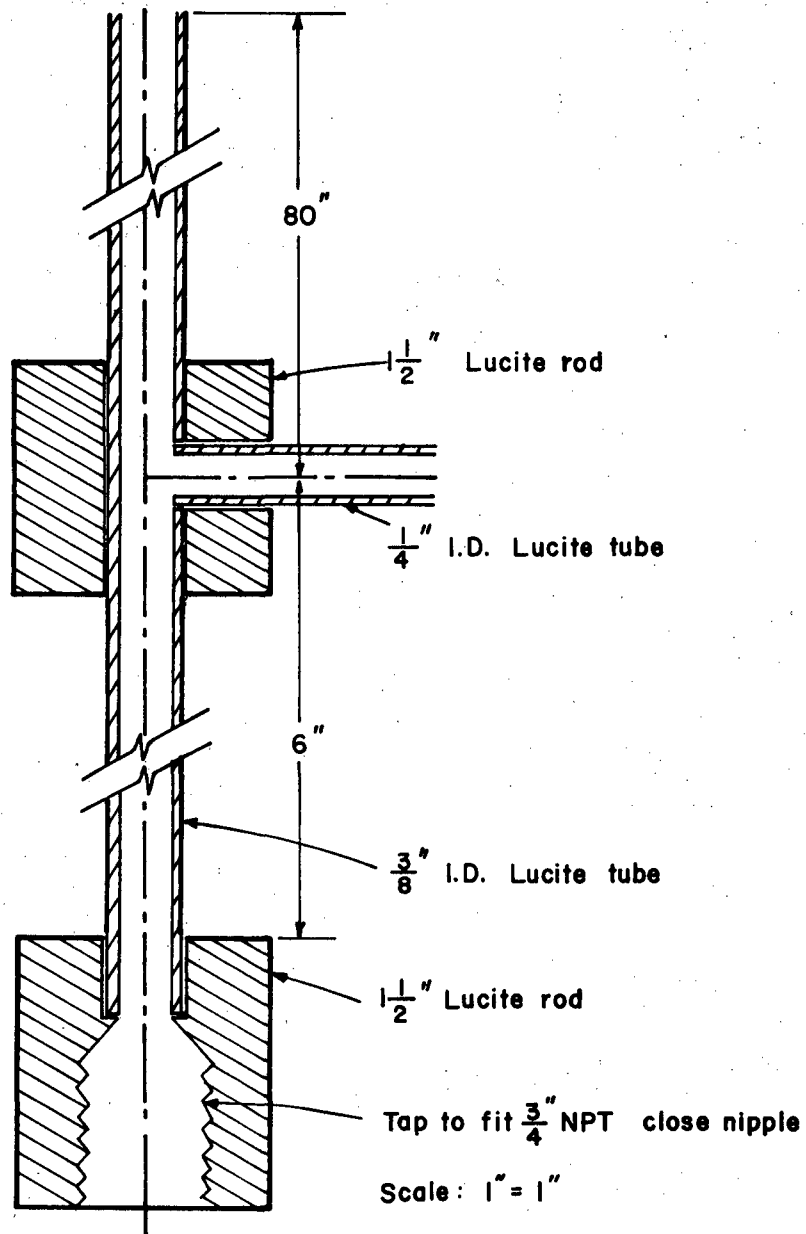
XBL 819-2001

Fig. 19. Flow curve for batch 7 used in penetration tests 13-21 as
determined with rotational viscometer.

$\tau_y = 505$ dyne $/cm^2$

XBL 819-2002

106
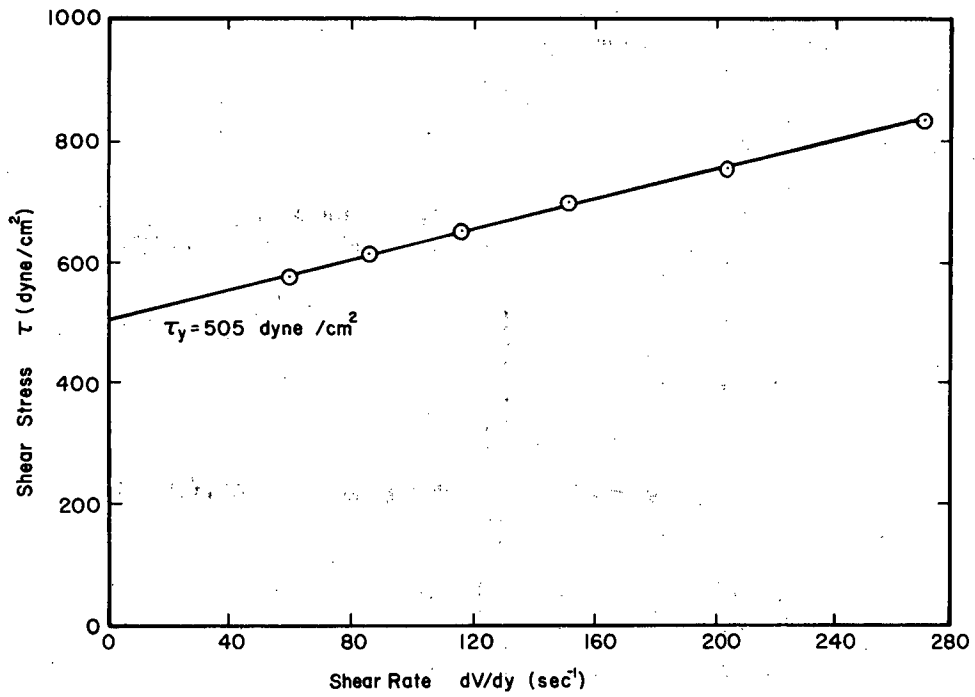
Fig. 20. Force balance on circular, vertical column of grout when flow

has ceased.

P_o = In situ pressure

τ_y = Shear stress at wall
when flow has ceased

$W = \gamma_g \pi R^2 L_{max}$

R = Radius of circular tube

L_{max}

P_i = Injection pressure $(P_i > P_o)$
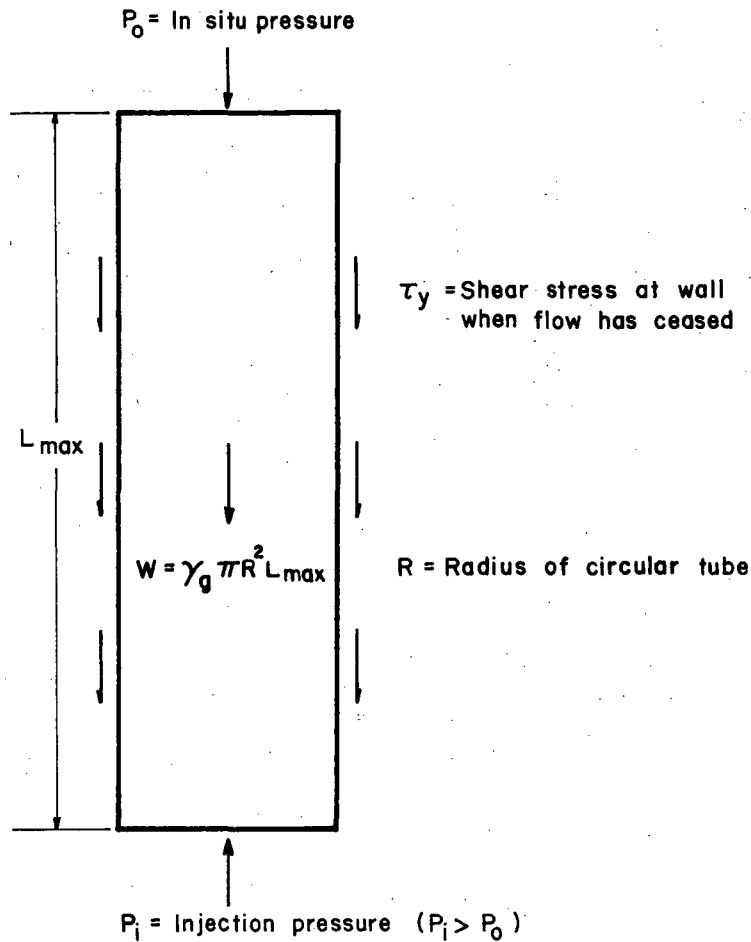
XBL 819-2003

Since $\sum F_y = 0$ when flow has ceased then

$$P_i \pi R^2 = P_o \pi R^2 + \tau_y \, 2\pi R L_{max} + \gamma_g \pi R^2 L_{max}$$

or

$$L_{max} = \frac{(P_i - P_o)R}{2\tau_y + \gamma_g R}$$

Fig. 21. Plot of L_{max}/R_H versus P_i/τ_y for circular penetration
tests.
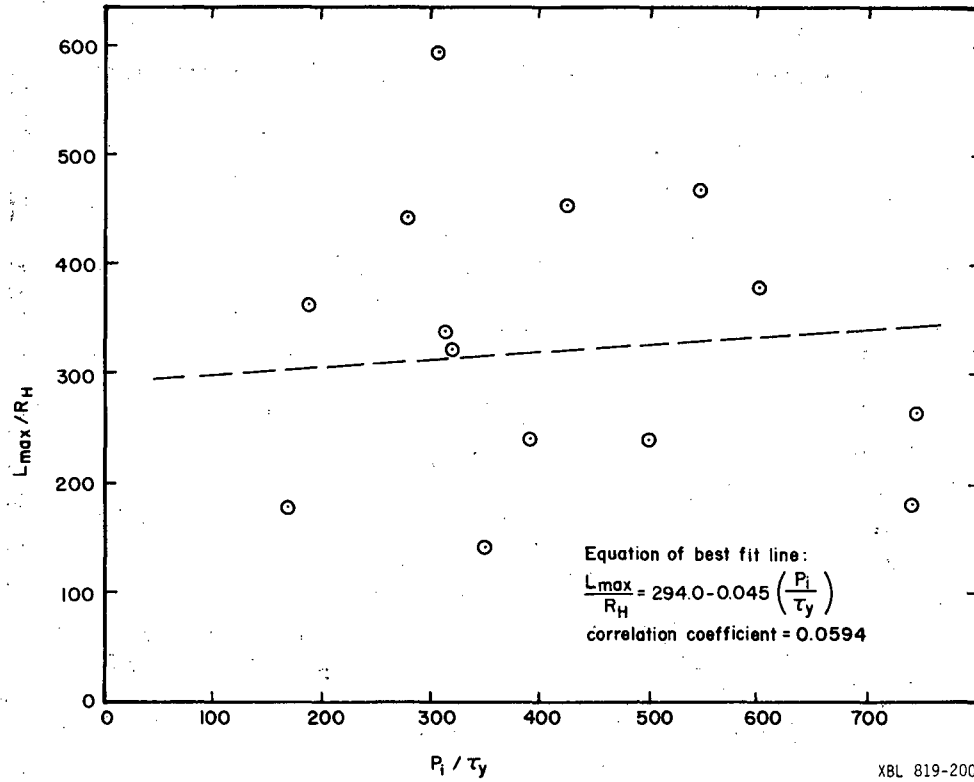
Equation of best fit line:

$$\frac{L_{max}}{R_H} = 294.0 - 0.045 \left(\frac{P_i}{\tau_y} \right)$$

correlation coefficient = 0.0594

XBL 819-2004

Fig. 22. Plot of L_{max}/R_H versus P_i/τ_y for penetration tests in triangular tubes.

Equation of best fit line:

$$\frac{L_{max}}{R_H} = 11.48 + 0.747 \left(\frac{P_i}{\tau_y}\right)$$

correlation coefficient = 0.930

P_i / τ_y

XBL 819-2005

Fig. 23. Plot of L_{max}/R_H versus P_i/τ_y for penetration tests in rectangular tubes.

Equation of best fit line:

$$\frac{L_{max}}{R_H} = -7.278 - 0.809 \left(\frac{P_i}{\tau_y}\right)$$

correlation coefficient = 0.998
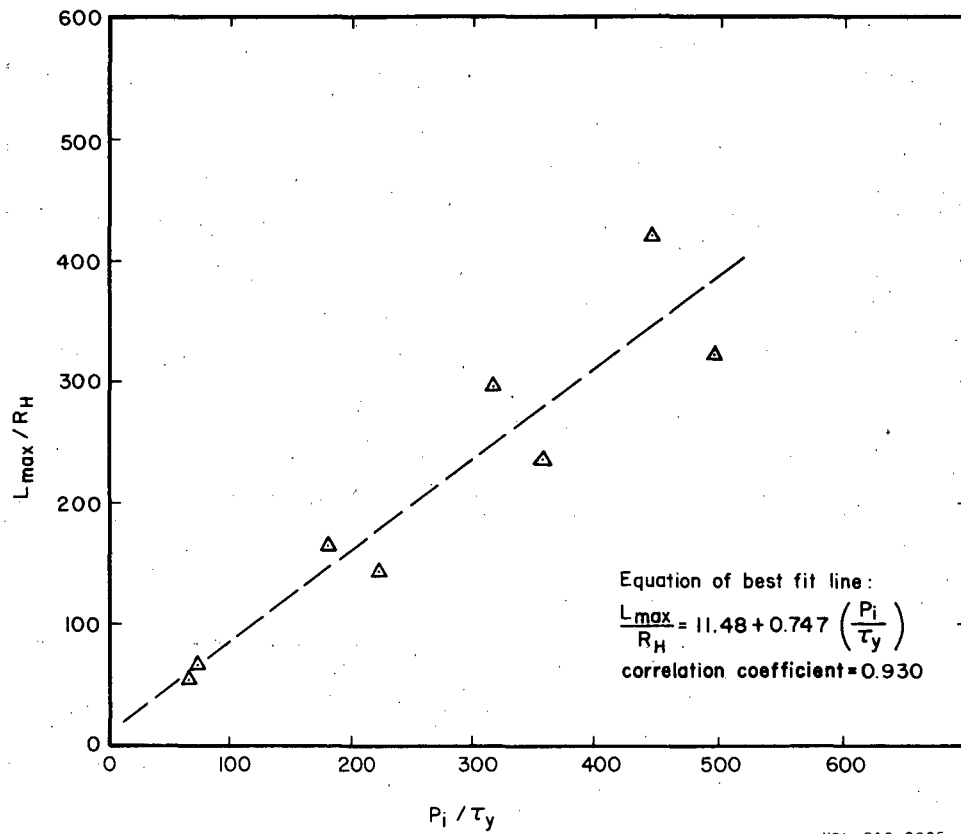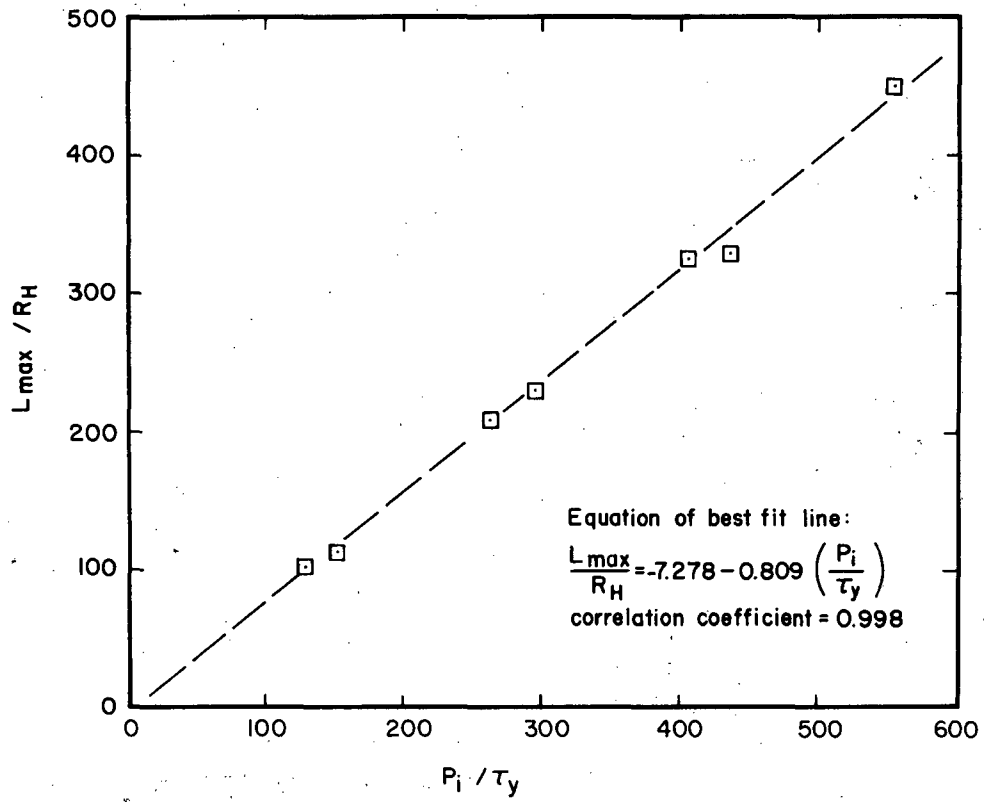
XBL 819-2006

Fig. 24. Plot of L_{max}/R_H versus P_i/τ_y for penetration tests in star-shaped tubes.

Equation of best fit line:

$$\frac{L_{max}}{R_H} = -5.60 + 1.315 \left(\frac{P_i}{\tau_y}\right)$$

correlation coefficient = 0.982

P_i / τ_y

XBL 819-2007
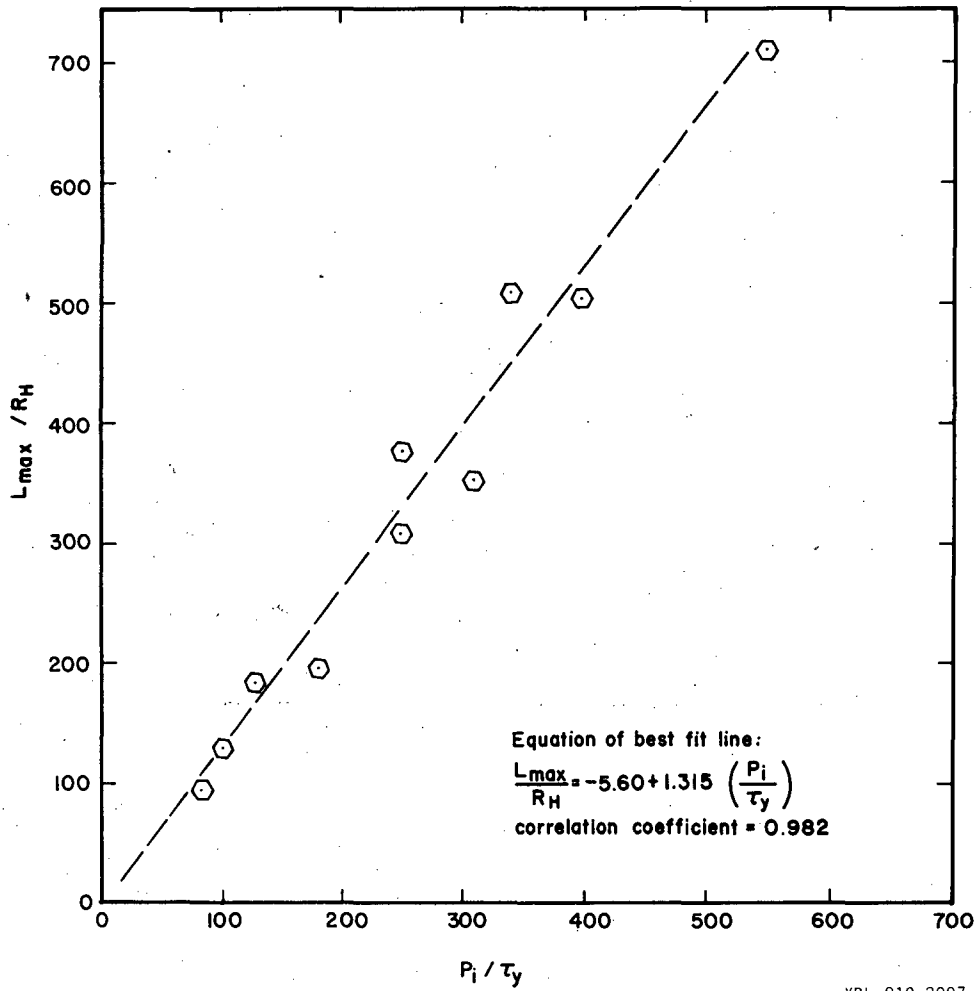
Fig. 25. Plot of L_{max} versus P_i for penetration tests in circular tubes.
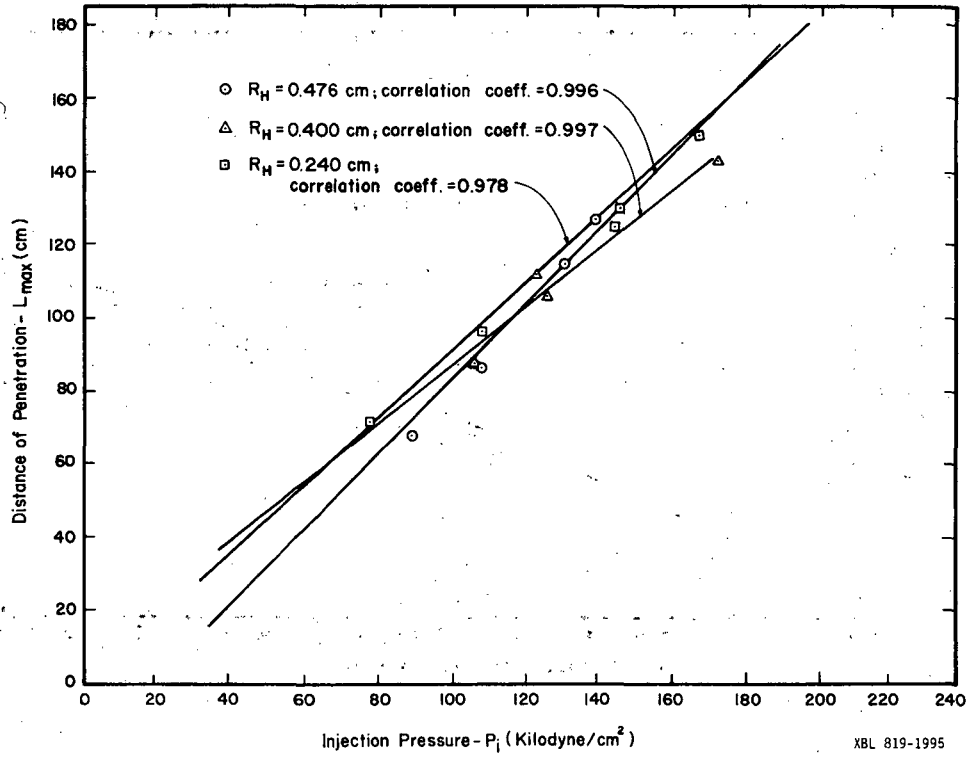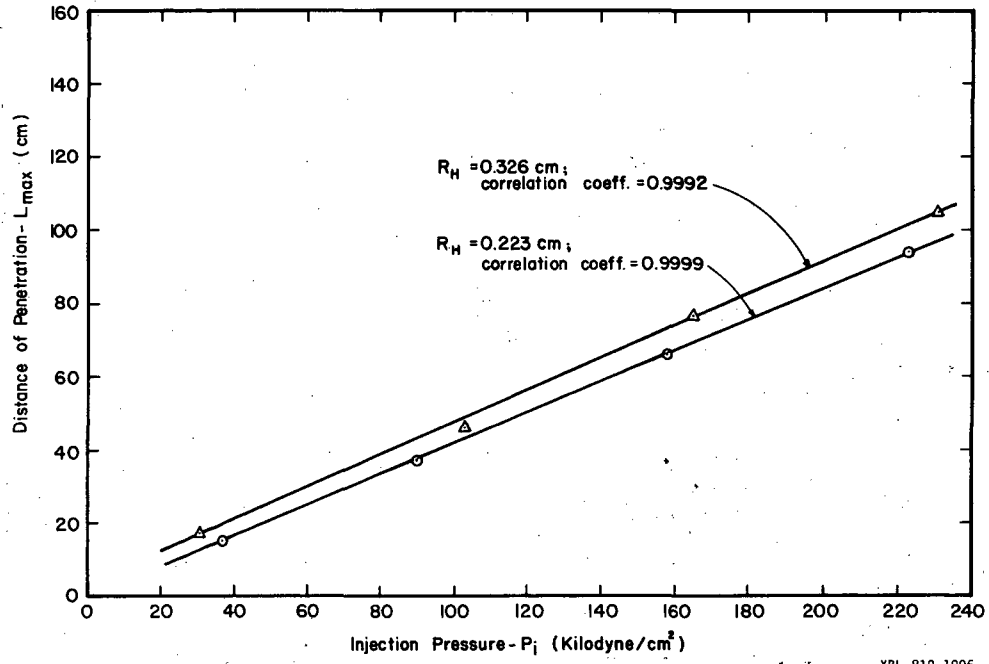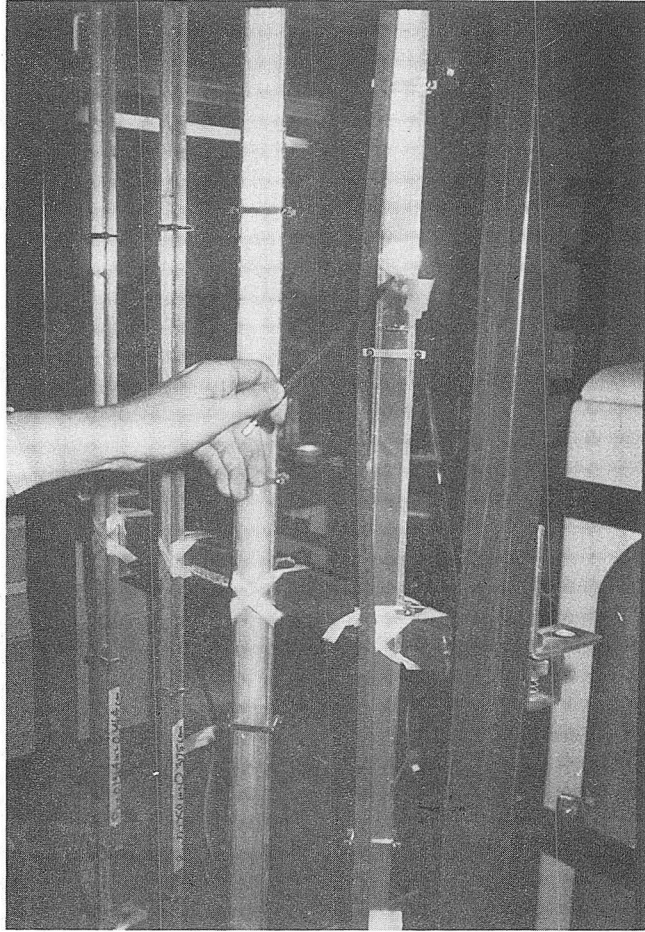

Distance of Penetration - L_{max} (cm)

○ $R_H = 0.476$ cm; correlation coeff. = 0.996
△ $R_H = 0.400$ cm; correlation coeff. = 0.997
▫ $R_H = 0.240$ cm; correlation coeff. = 0.978

Injection Pressure - P_i (Kilodyne/cm^2)

XBL 819-1995

Fig. 26. Plot of L_{max} versus P_i for penetration tests in
triangular tubes.

XBL 819-1996

Fig. 27. Plot of L_{max} versus P_i for penetration tests in
rectangular tubes.

Distance of Penetration - L_{max} (cm)

R_H =0.346 cm ;
correlation coeff. =0.9990

R = 0.318 cm ;
correlation coeff. = 0.9999

Injection Pressure - P_i (kilodyne/cm²)

XBL 819-1997

Fig. 28. Plot of L_{max} versus P_i for penetration tests in star-shaped tubes.

$\square$ $R_H = 0.261$ cm; correlation coeff. = 0.9996

$\triangle$ $R_H = 0.174$ cm; correlation coeff. = 0.9999

$\circ$ $R_H = 0.130$ cm; correlation coeff. = 0.9998

Distance of Penetration - L_{max} (cm)

Injection Pressure - P_i (kilodyne/cm^2)

XBL 819-1998
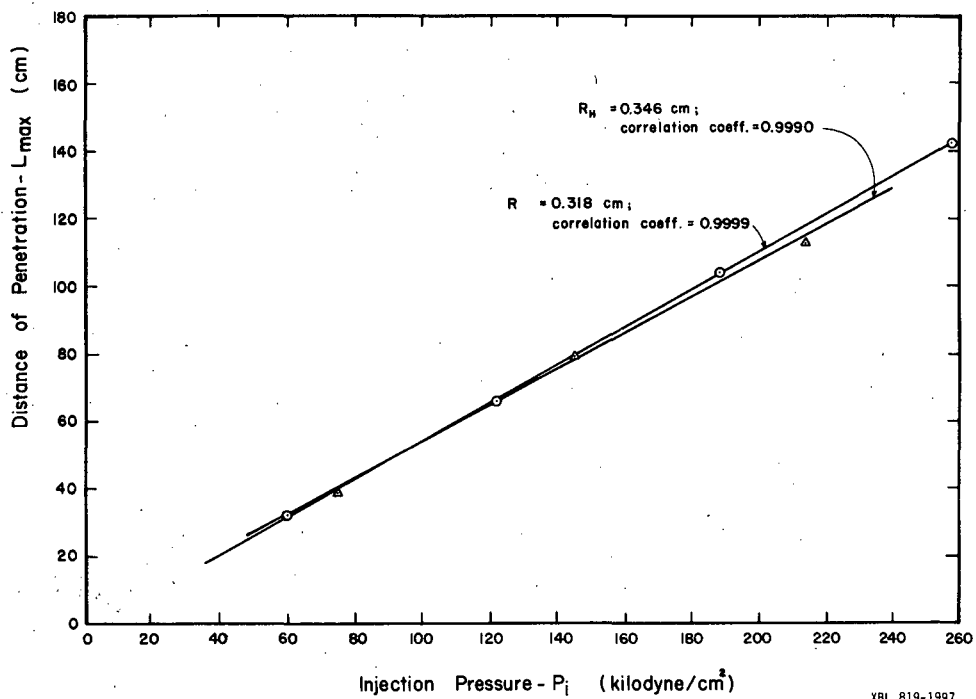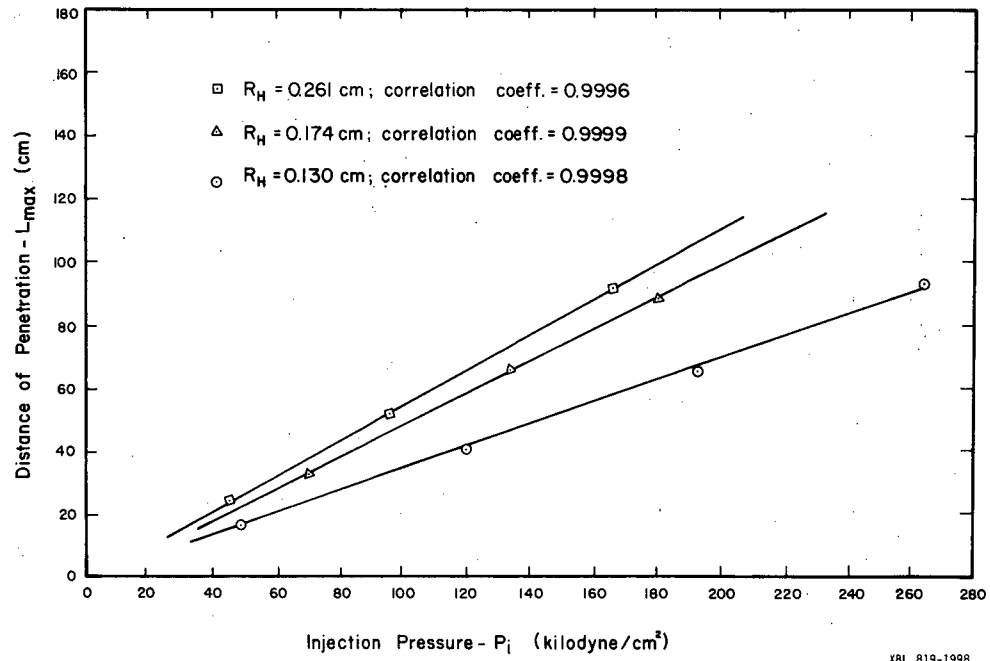
Plate 1. Pressure Tank and Reservoir
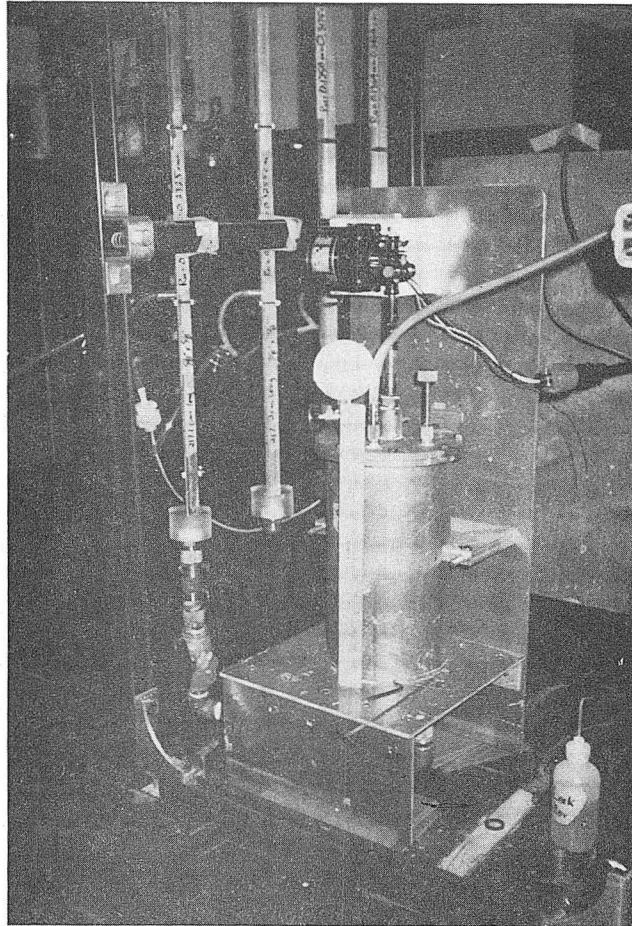
XBC 819-8681

Plate 2. Injection Tube.

XBC 819-8682

Plate 3. Pressure Transducer
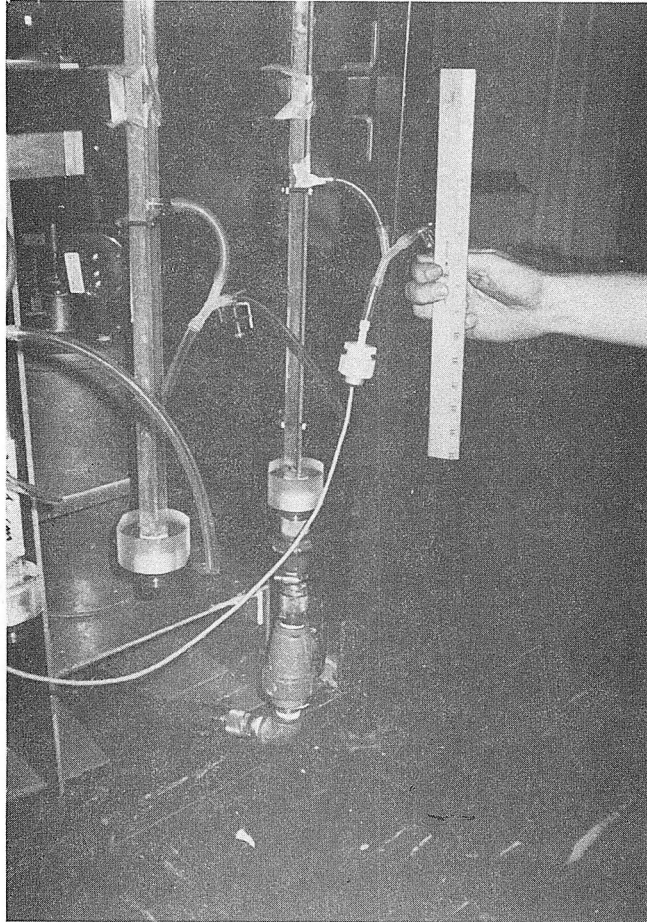
XBC 819-8683

Plate 4. X-Y Plotter.

XBC 819-8680

119
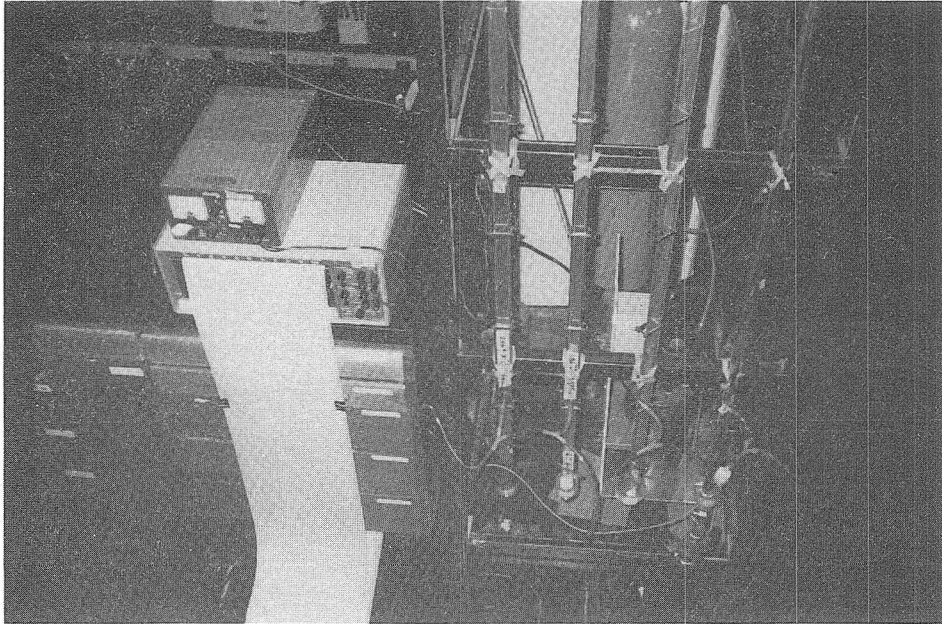
Plate 5. Complete experimental set-up as used in these tests.
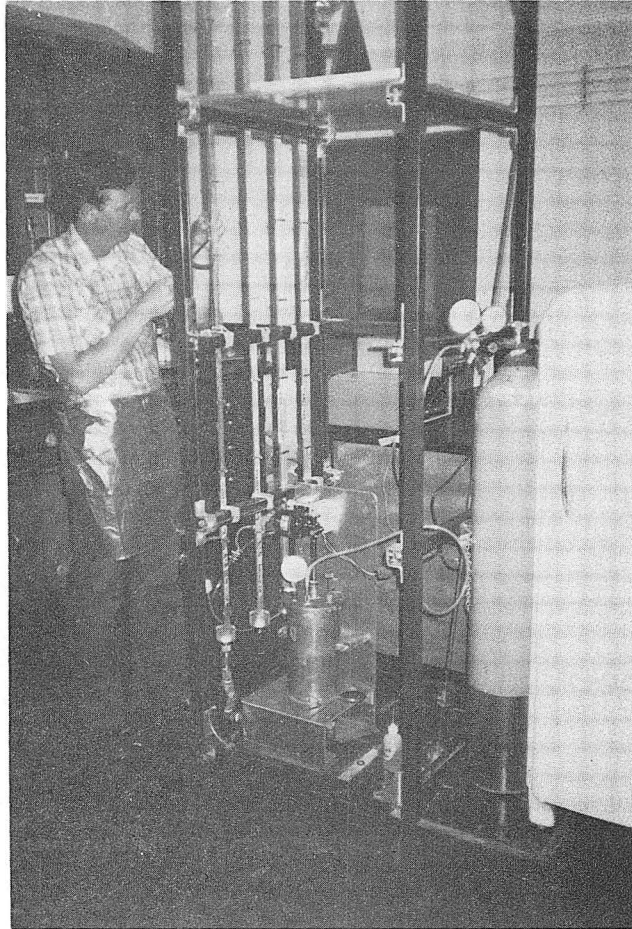
XBC 819-8679

TECHNICAL INFORMATION DEPARTMENT
LAWRENCE BERKELEY LABORATORY
UNIVERSITY OF CALIFORNIA
BERKELEY, CALIFORNIA 94720